

AD-A040 048

WISCONSIN UNIV MILWAUKEE DEPT OF GEOLOGICAL SCIENCES
MARINE GEOPHYSICAL INSTRUMENTATION.(U)
DEC 76 R J WOLD

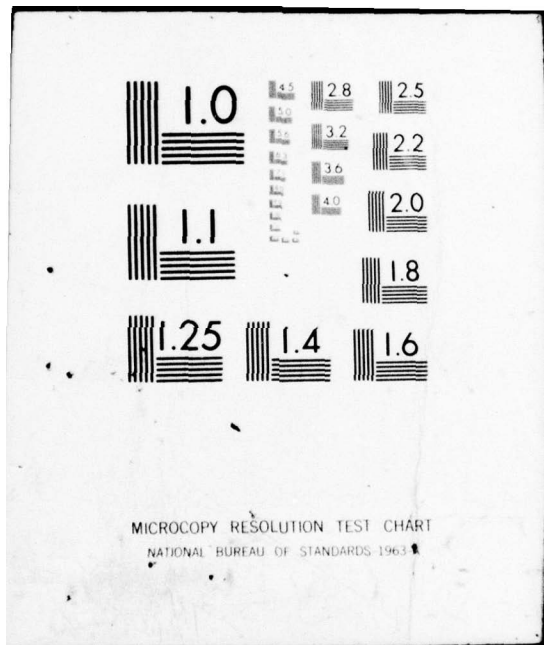
F/G 17/10

N00014-67-A-0128-0016
NL

UNCLASSIFIED

1 OF 2
AD
A040048





MICROCOPY RESOLUTION TEST CHART
NATIONAL BUREAU OF STANDARDS 1963-A

ADA 040048

Report N00014-67-A-0128-0016

12

J

MARINE GEOPHYSICAL INSTRUMENTATION

Richard J. Wold
Department of Geological Sciences
University of Wisconsin-Milwaukee
Milwaukee, Wisconsin 53201

COPY AVAILABLE TO DDC DOES NOT
PERMIT FULLY LEGIBLE PRODUCTION

31 December 1976

Final Report for Period 1 April 1970 thru 30 June 1976

DDC
RECEIVED
JUN 1 1977
RECEIVED

AY A -

AD No. 1
DDC FILE COPY

Prepared for
OFFICE OF NAVAL RESEARCH
Code 480
Naval Research and Development Activity
NSTL Station, Mississippi 39529

DISTRIBUTION STATEMENT A
Approved for public release;
Distribution Unlimited

REPORT DOCUMENTATION PAGE		READ INSTRUCTIONS BEFORE COMPLETING FORM
1. REPORT NUMBER N00014-67-A-0128-0016	2. GOVT ACCESSION NO.	3. RECIPIENT'S CATALOG NUMBER 9
4. TITLE (and Subtitle) 6 Marine Geophysical Instrumentation,		5. TYPE OF REPORT & PERIOD COVERED Final Report. 1 Apr 1970 thru 30 June 1976
7. AUTHOR(S) 10 Richard J. Wold		8. CONTRACT OR GRANT NUMBER(s) 15 N00014-67-A-0128-0016
9. PERFORMING ORGANIZATION NAME AND ADDRESS University of Wisconsin-Milwaukee Milwaukee, Wisconsin 53201		10. PROGRAM ELEMENT, PROJECT, TASK AREA & WORK UNIT NUMBERS
11. CONTROLLING OFFICE NAME AND ADDRESS Office of Naval Research, Code 480 Naval Research & Development Activity NSTL Station, Mississippi 39529		12. REPORT DATE 11 31 Dec 1976
14. MONITORING AGENCY NAME & ADDRESS (if different from Controlling Office) 12 116p.		13. NUMBER OF PAGES 116
		15. SECURITY CLASS. (of this report) Unclassified
		15a. DECLASSIFICATION/DOWNGRADING SCHEDULE
16. DISTRIBUTION STATEMENT (of this Report)		
<div style="border: 1px solid black; padding: 5px; width: fit-content; margin: auto;"> <p>DISTRIBUTION STATEMENT A Approved for public release; Distribution Unlimited</p> </div>		
17. DISTRIBUTION STATEMENT (of the abstract entered in Block 20, if different from Report)		
18. SUPPLEMENTARY NOTES		
19. KEY WORDS (Continue on reverse side if necessary and identify by block number) Magnetics, Marine Geophysical Instrumentation, seismics		
20. ABSTRACT (Continue on reverse side if necessary and identify by block number) In 1970, development was started on three marine geophysical instrumentation systems: a seismic recording and display system; a digital magnetometer system; and a magnetometer-gradiometer velocity system. In 1974, development was started on a Hydraulic-Pneumatic Water Gun. This report summarizes the development effort on each of these systems.		

406422

[Handwritten signature]

TABLE OF CONTENTS

	PAGE NO.
List of Figures	
Introduction	3
Digital Magnetometer System	3
Summary of Fiber-Optics Seismic Recording System (1971)	4
Seismic Recording and Display System (1972)	6
Seismic Recording and Display System (1973)	8
Hydraulic-Pneumatic Water Gun	14
Fiber-Optics Seismic Recording System	15
Interface Panel General Description	15
Interface Panel Power Supply	16
Interface Panel Pre-Processor Board	16
Interface Panel Variable Area Modulator Board	16
Interface Panel Time Varying Gain Board	17
Interface Panel Trigger Delay Board	17
Interface Panel Record Drive Board	18
Fiber-Optics Recorder Modifications	18
Current Status	19
Appendix I - Technical Specifications for Honeywell Recorder Model 1856A and Processor Model 1219	42
Appendix II - The Development and Evaluation of a New Marine Seismic Energy Source: The HP Water Gun	52

DESCRIPTION	
DTIC	White Section <input checked="" type="checkbox"/>
DDI	Def. Section <input type="checkbox"/>
UNANNOUNCED	<input type="checkbox"/>
RESTRICTION	
<i>letter on file</i>	
BY	
DISTRIBUTION/AVAILABILITY CODES	
Dist. AVAIL. and/or SPECIAL	
A 23 046	

LIST OF FIGURES

	PAGE NO.
Figure 1 - Digital Magnetometer System	20
Figure 2 - Three modes of recording seismic data on FOR	21
Figure 3 - Block diagram of off-line FOR System	22
Figure 4 - Effects of varying signal amplitude	23
Figure 5 - Honeywell Model 1218 magazine modified for Dry Silver Paper	24
Figure 6 - Σ modulation record run on modified 1218 magazine	25
Figure 7 - Standard seismic record run on EPC Model 4600 graphic recorder	26
Figure 8 - Infrared scanning record run on modified 1218	27
Figure 9 - Seismic record run on modified 1218 at 1.33 cm/sec. - Type 777 paper	28
Figure 10 - Seismic record run on modified 1218 at 3.2 cm/sec. - Type 777 paper	29
Figure 11 - Seismic record run on modified 1218 at 1.33 cm/sec. - Experimental Dry Silver Paper	30
Figure 12 - Seismic record run on modified 1218 at 3.2 cm/sec. - Experimental Dry Silver Paper	31
Figure 13 - Infrared scanning data recorded on Experimental Dry Silver Paper - Courtesy of Daedalus Enterprises	32
Figure 14 - Interface Panel (IP) Functional Block Diagram	33
Figure 15 - Schematic of IP chassis	34
Figure 16 - IP Front Panel Layout	35
Figure 17 - IP Pre-Processor Schematic	36
Figure 18 - IP Variable Area Modulator Schematic	37
Figure 19 - IP Time Varying Gain Schematic	38
Figure 20 - IP Trigger Signal Delay Schematic	39
Figure 21 - IP Record Drive Schematic	40
Figure 22 - Fiber-Optics Recorder modifications schematic	41

INTRODUCTION

The following report summarizes the effort under this contract from its inception April 1, 1970 to its termination June 30, 1976. The initial proposal was to develop three systems:

- 1) Seismic Recording and Display System
- 2) Digital Magnetometer System
- 3) Magnetometer - Gradiometer Velocity System

Later, in September 1974, development was started on a Hydraulic-Pneumatic Water Gun.

The summary of the efforts on each of these systems have been reported in the annual reports submitted each year as part of the proposal renewal. For example, the Digital Magnetometer System was reported in the first annual report. The final unit is shown in Figures 1 and 2. It measured 14"Hx21"Lx15"W and weighed about 35 pounds. It was capable of marine, airborne, or portable ground applications. It had a sensitivity of 0.5γ and read out directly in gammas. The system as shown in Figure 1 recorded on two Rustrak recorders and a paper-tape punch. The system was used to fly aeromagnetic surveys of parts of Montana, Utah, Wisconsin, and all of the state of Arizona as well as for marine studies in the Great Lakes and intermountain lakes of the west.

The annual summaries for the Fiber Optics Recording System are included here to show the development of the program.

SUMMARY OF FIBER-OPTICS SEISMIC RECORDING SYSTEM

(1971)

The following criteria were set up to evaluate the several possible approaches to data recording:

1. A graphic display of the seismic data is necessary.
2. There must be some improvement in the dynamic range of 22 db available on present graphic records.
3. The seismic display system must not be more expensive than the best commercially available unit.
4. The data must be available for study within a short period of acquisition.
5. It must be possible to monitor the data in real time.
6. It must be possible to display data in either an X-Y mode or variable density mode.

The biggest problem is the recording medium since it restricts the dynamic range of the system. The ideal system would use a color medium which would greatly expand the dynamic range. The best possibility would be to use a single gun type TV tube similar to that used by Sony. However, the optics and color film costs are prohibitively large.

The next best medium to color film is black and white film which is considerably cheaper. It offers a wider dynamic range than that available with dry or wet-paper type facsimile papers. It can be processed quickly, can provide a means of making additional copies and can be reduced or enlarged.

The next problem is to find some means of exposing the film with the seismic information. This first system proposed used a CRT and an optical system for photographing. The CRT is attractive from the standpoint of resolution and flexibility, however, the optics tend to be expensive. It was

then suggested that instead of a standard CRT, a fiber CRT be used. The Edo Western fiber optic recorder is a commercially available instrument, with a film magazine as an option, that fits the requirements. The resolution is 5-10 mils which is not as good as a standard high-quality CRT, however, the film is in direct contact with the CRT faceplate eliminating expensive optics and distortion inherent in a standard CRT.

Instead of using the variable intensity system available in the recorder a scheme would be utilized whereby a beam of constant intensity is turned on for a period of time which is proportional to amplitude. Since the cathode ray tube is photographed, the scheme is analogous to that utilized by a camera. By using a photomultiplier or other light detector, a closed loop system is possible which will compensate for variations in beam intensity due to power supply fluctuation, component aging, etc. This time-intensity system coupled with the capabilities of photographic film offers a large dynamic range and should provide information unattainable by existing systems.

The recorder also allows the possibility of recording in the X-Y mode. This could be done in real time simultaneous with variable density display (the two traces would follow each other on the same sweep). An alpha-numeric CRT is also built into the recorder allowing direct notation on the photographic film.

Several problems exist with the photographic film that need further investigation:

1. How fast can the film be processed? Possibly the Kodak Bimat process could be used. The main problem is that Kodak may not continue making Bimat film.
2. What will the time delay be between the film exposure and its availability for viewing? This could be quite large at slow "chart" speed.

Since a new recording system is needed, is there some way to build the recording system to help in data analysis? There is a considerable amount of routine in interpretation which the recording system might help. One possibility is to use the duration of time-intensity modulation to identify the bottom reflection (usually a large amplitude signal) and to identify major sub-bottom reflections. The time between these events in a single trace might be recorded on tape and/or played onto another graphic recorder. Following this approach maybe traces could be built up on a monitor scope and major reflections identified. A variable spot could be moved across the face of the tube and aligned with a reflection of interest. By pushing a button the duration of the particular time-intensity modulation could be read out or fed back into the system to be recorded on the special recorder for further analysis.

SEISMIC RECORDING AND DISPLAY SYSTEM

(1972)

A Honeywell Model 1856 Fiber optics recorder was obtained along with a film magazine so that photographic as well as dry-write paper could be used. This basic recorder has a usable fiber bundle 12 cm wide by 1 cm high.

It has been possible to record marine seismic profiling data in the X-Y mode (Fig. 2a), the X-Y-Z mode (Fig. 2b), and the X-Z mode or variable density mode or variable density mode similar to the standard graphic recorder.

It has been possible to replay seismic data, recorded on magnetic tape at 1 7/8 ips, with speeds of 15 ips. If a tape recorder capable of 60 ips were available, there is no reason it wouldn't be possible to replay data at those speeds. This would mean a 3600' tape, which requires six hours to record at 1 7/8 ips, could be reprocessed in 12 minutes at 60 ips.

Several additions should be added to the basic fiber-optics recorder.

These are:

- 1) Crystal controlled sweep and paper advance. Also a control will be provided so that paper advance is in terms of sweeps/cm.
- 2) Delayed sweep will be added ranging from 10-100 ms. and 1-10 secs.
- 3) Using the built in record number marker, a modification will be added so that the numbers are recorded according to an external timing system, i.e., every minute or five minutes, etc.
- 4) A data recording module will be adapted that will allow the data to be recorded on the 3M dry silver paper. This paper must be developed with heat but it gives a record which is insensitive to storage, pressure, or moisture.

A unique capability of the fiber-optics recorder is its high speed. Data may be replayed through the system up to 32 or possibly 64 times its initial recording speed. Different filters and gain techniques may be employed on the playback to enhance the data. The biggest problem appears to be amplifiers and filters since the data frequencies are also 32-64 times their original values. It is particularly a problem with automatic gain controls or time varying gains since the attack rate on most amplifiers is too low. A couple of commercially available amplifiers will be evaluated.

In order to best utilize the unique features of the fiber-optics recorder it should be an "off-line" system. A standard dry paper graphic recorder would be used for real time recording with the fiber-optics recorder and an associated data processing system being used to reprocess data at high speed.

Some of the things that might be done "off-line" would be elimination of multiples and bubble pulse, cross-correlation and summing of adjacent traces, re-filtering, and using different methods of gain control. A possible block-diagram of such a system is shown in Figure 3.

It is proposed to investigate the possibility of constructing such a system. There are several possibilities for the data processing system which should be checked before a system is constructed.

It is essential to be able to directly compare the fiber-optics recorder and a dry paper graphic recorder. We propose to purchase one of the new low price dry paper models.

SEISMIC RECORDING AND DISPLAY SYSTEM

(1973)

The application of the Honeywell Model 1856 fiber-optics recorder for recording marine seismic profiling data has been evaluated further. In general, the fiber-optics recorder performs very well for recording seismic data.

Some problems were encountered with the recorder at very low record speeds. When using photographic film, it was found that there was a small light leak from the photo cell timing line generator. After consultation with Honeywell, a modification was developed to eliminate this problem. Another problem at low speeds was that, in the triggered record drive mode, the line spacing was uneven. The solution to this problem was to run the record drive motor at higher speeds and gear down the output. The problem might also be resolved by using a stepping motor to drive the record. Another problem was the inability to change the polarity of the input signal on the Z-axis modulation or to eliminate DC levels that might exist on the input. However, since the recorder was delivered in 1972, Honeywell has developed a new Video Input Circuit Card to replace the Blanking Amplifier. This provides polarity, contrast, and do offset control on the Z-axis input.

Other problems encountered relate to the level of the input signal. The overall signal level is particularly critical when the signal is applied simultaneously to the vertical and Z-axis (XYZ mode). Figure 4 illustrates this

problem. The far right side had an average signal recorded on tape of a considerably larger magnitude than the left side. The amplitudes of the trace are increased resulting in an excessive overlap from one trace to the next and a smearing effect results. A solution to this problem would be either constant monitoring of the input signal level or design of an appropriate AGC circuit.

The major effort of the past year has been devoted to a study of the various recording films and papers. The major disadvantage of the Honeywell recorder was the restriction of using either direct print paper or photographic mediums requiring wet processing in a darkroom. The direct print paper allows rapid viewing of the data but the paper has a limited gray scale range and is unstable with time. The photographic films and papers have a wide grade scale range, are stable with time, but do not allow rapid viewing. The best compromise appeared to be the 3M Dry-Silver papers and films. They offer a wide gray scale range, good resolution, good stability with time and rapid viewing. The only problem is that they must be developed with heat.

In order to evaluate the dry silver products, a 3M processor and Type 777 paper was obtained. Paper was exposed on the recorder using the Honeywell Model 1218 Film Magazine and developed in the darkroom on the 3M processor. The Type 777 paper has its greatest sensitivity to the blue-green area, whereas the Honeywell 1856 Recorder has a P16 phosphor which is in the violet and near-ultraviolet range. The preliminary tests, however, indicated that the 3M Type 777 paper performs quite well on the 1856 Recorder. The limitations would probably come at extremely high speeds, beyond that of interest for the seismic application.

The next step was to modify the Honeywell 1218 Film Magazine to process the 3M Dry-Silver paper directly. Figure 5a shows the modified 1218 Magazine attached to the front of the recorder. Figure 5b shows the magazine alone.

The modification to the magazine involved adding a heating element to the front of the magazine. The heating element is a 1-1/2" copper tube (Fig. 5c) with a 1000 watt calrod unit inserted inside the tube. Heat conduction from the calrod unit to the copper tube is through aluminum chips which fill the gap between the calrod heater and the copper tube. The copper tube is covered with a thermal blanket to maintain a constant heat across the copper tube. The take-up reel has been modified so that the paper is pulled through with the take-up motor in the magazine and fed out the top of easy viewing. If desired, this take-up arrangement may be removed and the regular take-up reel inserted (Fig. 5d).

The temperature is controlled by means of an automatic temperature controller which will be attached to the left side of the magazine.

An example of a seismic record run with the 1856 recorder and modified processor is shown in Figure 4. This record was run in the XYZ mode. An example of a standard Z modulation record is shown in Figure 6. The left side of Figure 6 indicates a fair amount of noise due to excessive external electronic noise in the trigger channel. Figure 7 is a sample of a standard record run on an EPC Model 4600 graphic recorder.

In order to explore the full potential of the processor, several different types of data were run with the 1856 recorder and processor. Figure 8 is an example of infrared scanning data over a marsh in northeastern Wisconsin.

Several tests were run to check the capabilities and limitations of the modified processor and the 3M Dry Silver paper. In February (1973) a Honeywell engineer and the principal investigator ran several tests with the Type 777 paper and an experimental glossy paper developed by 3M. The processor was capable of operating from .016 cm/sec to 3.2 cm/sec, a speed range of 200:1. The low speed limitation is partly a function of how slow the recorder could go in the continuous record drive mode. The records in Figures 6 and 7 were

run at .016 cm/sec. An example at 1.33 cm/sec is shown in Figure 9 and at 3.2 cm/sec in Figure 10. These records were recorded on Type 777 paper. Figures 11 and 12 illustrate the same speeds on the experimental paper. The experimental paper provides excellent resolution but has a very narrow range from white to black. An example of a different 3M experimental paper which does seem to have a wide gray scale range is shown in Figure 13. This is a record of scanning data recorded by Daedalus Enterprises Inc., on a 1856 recorder.

The studies on the 3M Dry Silver paper indicates that it can be developed over a wide range of conditions. The modified Honeywell magazine provides contact between the paper and heat source for about 1/2 cm. This means that at .016 cm/sec the paper is in contact with the heat source for about 30 seconds, whereas at 3.2 cm/sec the paper is in contact for only 150 msec. This considerably exceeds the specifications listed by 3M for the Type 777 Dry-Silver paper. The studies also imply that by increasing the contact area the speed could be increased. For instance, with a contact length of 1 cm the recording speed could be doubled to about 6 cm/sec, which far exceeds the requirements for seismic recording but may be useful for high frequency acoustic studies.

Since the Honeywell recorder does not have a delay trigger, a delay unit was built that provides a delay up to 10 sec in 1 msec intervals.

Two modifications proposed last year will be added. These are:

- 1) Crystal controlled sweep and paper advance. Also a control will be provided so that paper advance is in terms of sweeps/cm.
- 2) Using the built-in record number marker, a modification will be added so that the numbers are recorded according to an external timing system, i.e., every minute or five minutes, etc.

It had been proposed to utilize some form of digital processing to analyze the seismic data before replaying on the fiber-optics recorder. After additional investigation it appears that the hardware and software costs would be excessive.

The principal investigator feels that more can be done with analogue systems than has been. Along this line some of the currently commercially available seismic amplifier systems are being evaluated. If any of these systems appear to be useful, it is proposed to purchase it and proceed with additional development.

A problem common to all seismic display devices is that the dynamic range of the display is less than that of the signal. The signal must, therefore, undergo a conditioning process with a minimum sacrifice of information. For a real time processor, it is necessary for the amplifier gain controller (AGC) to operate on a running average of the output signal amplitude of the processor. The averaging process is performed by some form of low pass filter, acting upon the output of some form of detector.

In the case of a wide band amplifier (20 Hz to 20 KHz) too rapid an AGC action will destroy low frequency components of the signal, and at the same time, may not be rapid enough to act upon the high frequency components. This would imply that the AGC reaction time should be a function of signal spectrum. An optimal AGC system then, should have the capability to adapt its reaction time to the spectrum of the information being processed. In this way, the maximum available dynamic range of the display is always utilized.

The heat processor modification for the Honeywell magazine will be improved. 3M has offered to work with us on this and will be sending an engineer to evaluate the processor. In addition, they will be sending more experimental films and papers for testing. Their films have not been tested yet but they offer the advantage of quick access and the ability to be blown up.

The types of outputs available on the fiber-optics recorder have not been fully analyzed. Some of these possibilities are:

- 1) Signal applied to the Z-axis only on Z modulation (XZ mode).
- 2) Signal applied to the Y-axis only such that the vertical deflections are proportional to the signal strengths (XY mode).
3. Signal simultaneously applied to the vertical and Z-axis, resulting in intensifying the trace at the peaks of the vertical deflection (XYZ mode).
4. All of the following are in the XYZ mode:
 - a) Output from standard amp. on Y.
Output through time varying gain (TVG) on Z.
 - b) Output from AGC amp. on Y.
Output from TVG amp. on Z.
 - c) Different filters setting to Y and Z simultaneously.

It is the purpose of this final report to summarize the activities since the last annual report submitted for the time period June 1, 1973 - June 1, 1974.

Hydraulic-Pneumatic Water Gun

The implosive generation of seismic energy offers inherent advantages over explosive techniques. Explosive generation of seismic energy results in considerable energy remaining in the bubble/afterflow system after initial signal generation. Oscillations of the bubble result in secondary events of the radiated acoustic signal. Attenuation of the secondary effects or bubble pulse requires large arrays of energy sources or significant loss in radiated acoustic energy.

Implosive generation of seismic energy uses the collapse of a vacuum volume to generate a broad band, high amplitude acoustic pulse. The transfer of energy from the source to the marine environment must be a relatively long-term process relative to explosive methods. A long-term transfer of energy allows the use of mechanisms not practical in explosive techniques.

The system developed at the University of Wisconsin-Milwaukee uses the implosive generation of seismic energy coupled with a highly efficient restoring mechanism. Dynamic characteristics inherent in the vacuum volume generation allow the use of a hydraulic/pneumatic restoring mechanism. The use of a hydraulic system as the prime energy transfer mechanism coupled with a low compression, high pressure pneumatic system results in an extremely efficient system.

This system development and evaluation was reported by Bill L. Jaworski as his Master of Science thesis at the University of Wisconsin-Milwaukee. A copy of this thesis is contained in Appendix II.

Fiber-Optics Seismic Recording System

The fiber-optics recording system is composed of a Honeywell Model 1856A Oscillographic recorder, Honeywell Model 1219 photographic processor, and an Interface Panel (IP).

The Technical specification for the Model 1856A recorder and Model 1219 Processor are listed in Appendix I.

IP General Description

Figure 14 shows a functional block diagram of the Interface Panel for the Fiber-Optic Recorder. A seismic signal coming into the unit enters the pre-processor (P-P) board. It goes through a linear amplifier and then goes either to the output of the P-P board or back into the P-P board where the signal is fed into a voltage logarithmic amplifier. The output (linear or log) from the P-P board can either be switched to the signal output from the Interface Panel, the Time Varing Gain (TVG) board, the Variable Area Modulator (VA) board, or both TVG and VA.

The trigger input for the Fiber-Optic Recorder (FOR) is fed into a Time Delay Board which can delay the trigger from 1 msec to 9.999 sec. The trigger output to the FOR is also fed into the TVG Board to start TVG action.

The last major function contained in the Interface Panel is the motor drive board. This board contains the circuitry to drive the stepping motor inside the FOR which advances the recording paper.

In addition, FOR controls have been brought out to the Front Panel. These include record number select, recorder number reset, timing line select, and timing line mark.

A schematic of the Interface Panel wiring is shown in figure 15. The front panel layout for the interface unit is shown in figure 16.

IP Power Supply

The D C voltages required +5, +12, +15, and -15 are provided by Powertec sub-modules. The +5v supply is a Powertec module 22B-100 and it receives its A C input from a Stancor P8388 transformer. The +12v, +15v, and -15v supplies are Powertec modules 22B-300. They all receive their input from a Powertec model PT-22C transformer.

IP Pre-Processor Board

The Pre-Processor Board circuitry is modified from circuitry developed at Lamont-Doherty Geological Observatory for a Fiber-Optic Scope Control. The P-P Board as shown in Figure 17 contains a linear amplifiers and a voltage logarithmic amplifier is a Teledyne Philbrick Model 4350 log module.

The only internal control on the P-P Board is a 10k offset null pot. External controls shown in Figure 16 include a function switch to select either positive or negative components of the input signal on a position which allows the entire signal to be amplified. A 50k attenuation control is also available in the linear amplifier section of the board. A switch is available to select either the linear output from the board or the logarithmic output which in effect feeds the signal back into the board where it is acted upon by the Philbrick 4350 log module. Front panel controls in the log amplifier section include a log contrast pot. The overload LED is monitoring the output from the P-P Board in both Linear and Log modes.

IP Variable Area Modulator Board

The Variable Area Modulator Board circuitry is modified from circuitry developed at Lamont-Doherty Geological Observatory for a Fiber-Optic Scope Control. The VA Board shown in Figure 18 contains a VCO, four quadrant multipliers, and operational amplifiers (EXAR XR-5200 and Motorola MC 1494L). The incoming seismic signal is amplitude modulated with a 50 KHz carrier.

The internal controls on the VA Board include a null and symmetry control which controls the carrier output level and symmetry of the output waveform. Carrier symmetry and amplitude controls are also available. No external controls for the VA Board are contained on the interface panel.

IP Time Varing Gain Board

The time varying gain board circuitry is modified from circuitry developed at Lamont-Doherty Geological Observatory. The TVG board shown in Figure 19 contains a timer, four quadrant multiplier, and operational amplifiers. The circuit varies the gain on the incoming seismic signal according to the settings of controls on the front panel. The TVG is initiated upon receiving a trigger pulse from the time delay board.

Internal controls on the TVG board include a pair of 10k balance pots. External controls on the front panel include a gain control on the signal output. Slope and duration controls are available for setting the rate of gain change and the length of time over the gain changes.

IP Trigger Delay Board

The trigger delay board shown in Figure 20 contains a 500KHz crystal controlled oscillator, operational amplifier, nand gates, decade dividers, and BCD-to-decimal decoders. The circuit delays the incoming sweep trigger signal by an amount determine by switch settings on the front panel. This trigger delay is sent on to the fiber-optic recorder to initiate the sweep and the trigger delay is sent to the TVG board.

Internal controls on the time delay board include an oscillator drive, incoming trigger gain, and incoming triggler duration. External controls on the front panel include a reset button and a 4 digit switch to set the delay from between 1 msec and 9.999 sec. in 1 msec steps.

IP Record Drive Board

The record drive board shown in Figure 21 contains a function generator whose frequency is controlled by switches on the front panel. The function generator output is fed into circuitry which provides the drive pulses for a slo-syn synchronous motor.

External controls on the front panel include a coarse and fine speed adjust calibrated in cm/sec. The key or continuous run switch allows the unit to drive the motor continuously at a rate determined by the speed adjust controls. In the key position the paper will only be advanced when it received a pulse from either an external source or internally from the blanking pulse output of the fiber-optics recorder, depending upon the setting of the Int-Ext. switch. Therefore, with the switch set on Int., the paper will advance only after the Fiber-Optic Recorder has received a trigger pulse and the electron beam swept across the Fiber-Optic Scope face.

Fiber-Optic Recorder Modifications

Figure 22 shows the wiring additions inside the FOR. The constant velocity servo drive system in the FOR was removed (motor and tachometer) and replaced with a Slo-Syn Model SS25-1001 synchronous motor. As shown in Figure 22 the Slo-Syn motor is used as a stepping motor. The remaining wiring additions were done in order to bring various FOR function controls to the interface panel for easier access. The figure and page numbers referenced on Figure 22 refer to the Honeywell Technical Manual for the Model 1856 recorder.

One additional modification that has been made to the FOR is not electronic. It involves removing the piece of film that is the faceplate overlying the flashtube which generates the reference lines. The transverse reference line on the film is blacked out between the horizontal reference markers spaced 1 cm apart.

Current Status

February 1, 1975, the principal investigator and writer of this report took a one year leave-of-absence from the University of Wisconsin-Milwaukee. In February, 1976, this separation was made permanent and the principal investigator is now with the U. S. Geological Survey Office of Marine Geology in Woods Hole, Mass. Because of this physical separation from the University of Wisconsin-Milwaukee and, therefore, the necessary technical support and equipment, it became very difficult to properly complete the instrumentation.

In June, 1976, a prototype Interface Panel, model 1856A and 1856 Honeywell recorders, accessories, film processors, etc. were sent to:

Martin Fagot
Naval Ocean Research and Development Activity
Naval Oceanographic Lab (Code 351)
Bay St. Louis, Mississippi 39520

No communication has yet been received from the NORDA group concerning the present status of the Fiber-Optics Seismic Recording System.

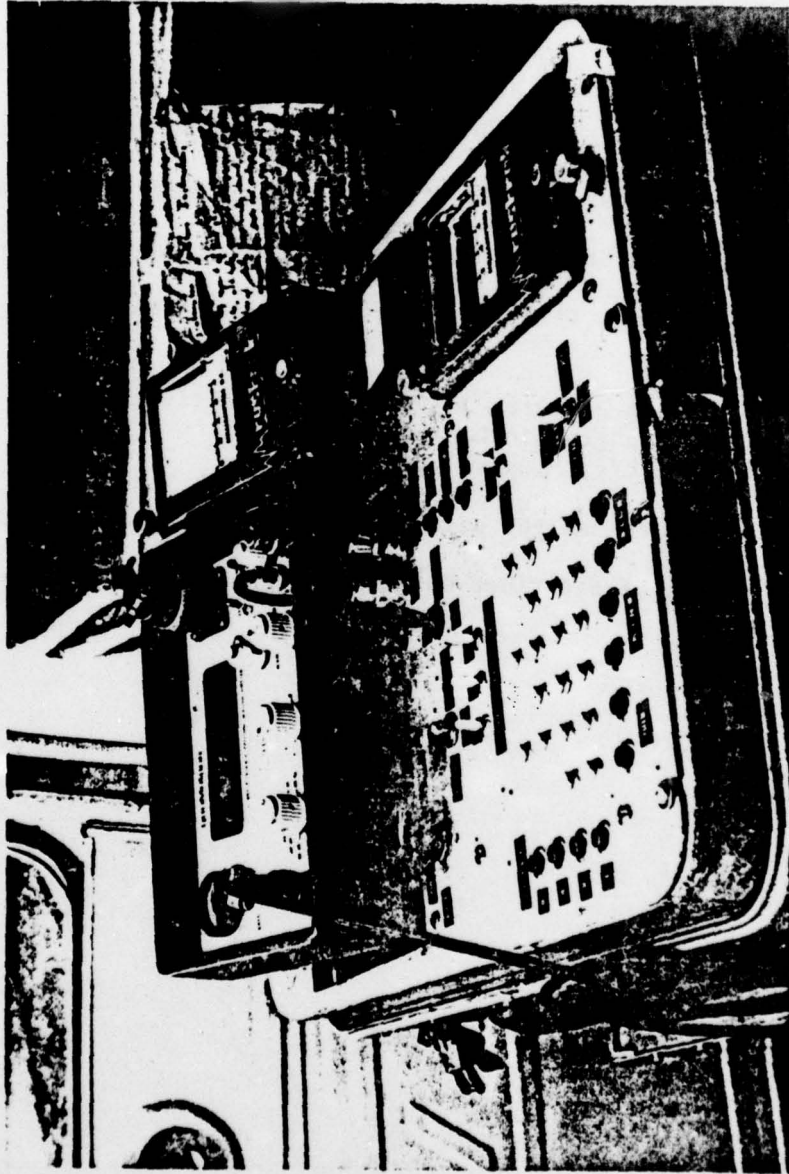


FIGURE 1

Seismic data recorded at 1 7/8 ips and replayed at 15 ips. Vertical Time Scale = 40 ms/cm.

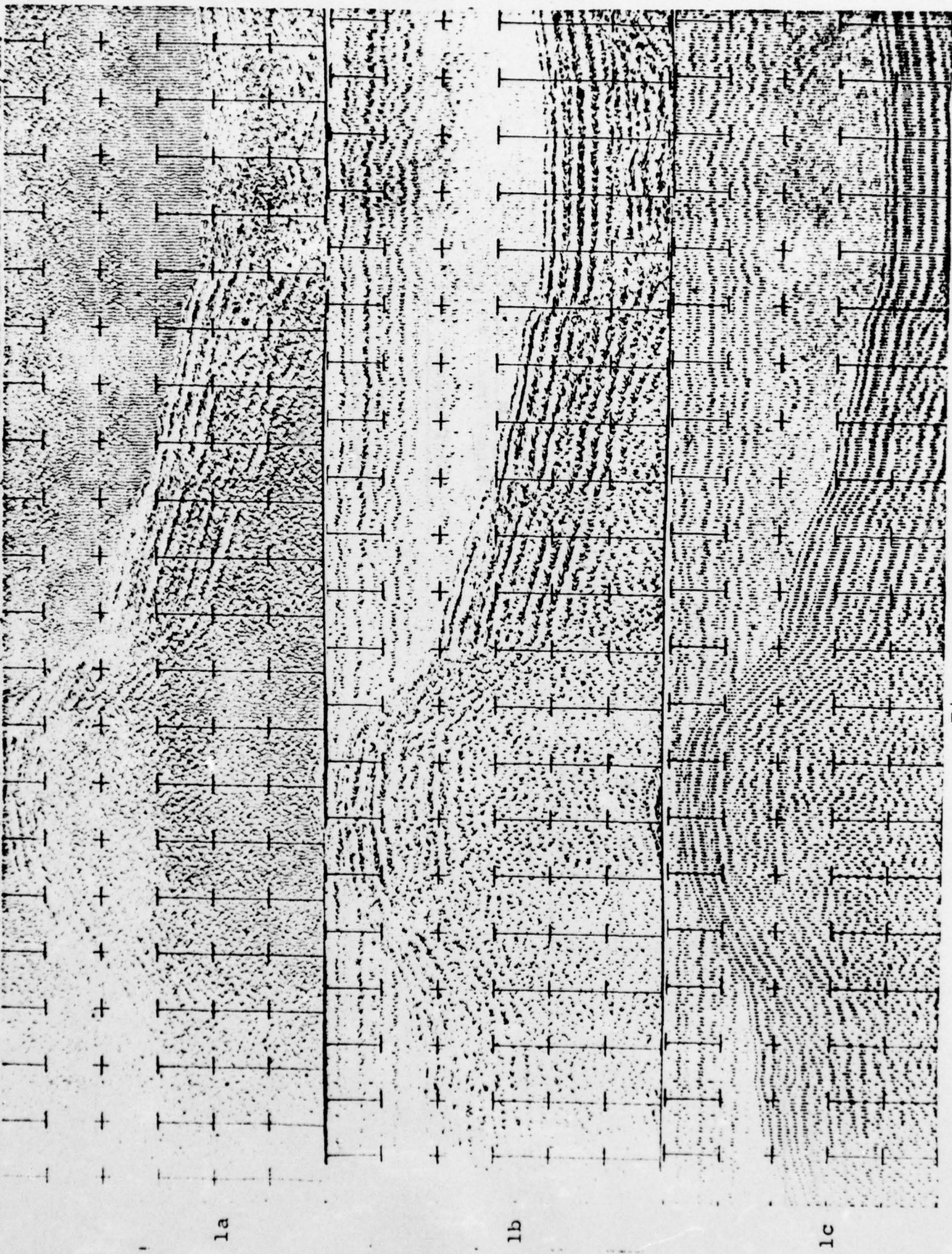


Figure 2

BEST AVAILABLE COPY

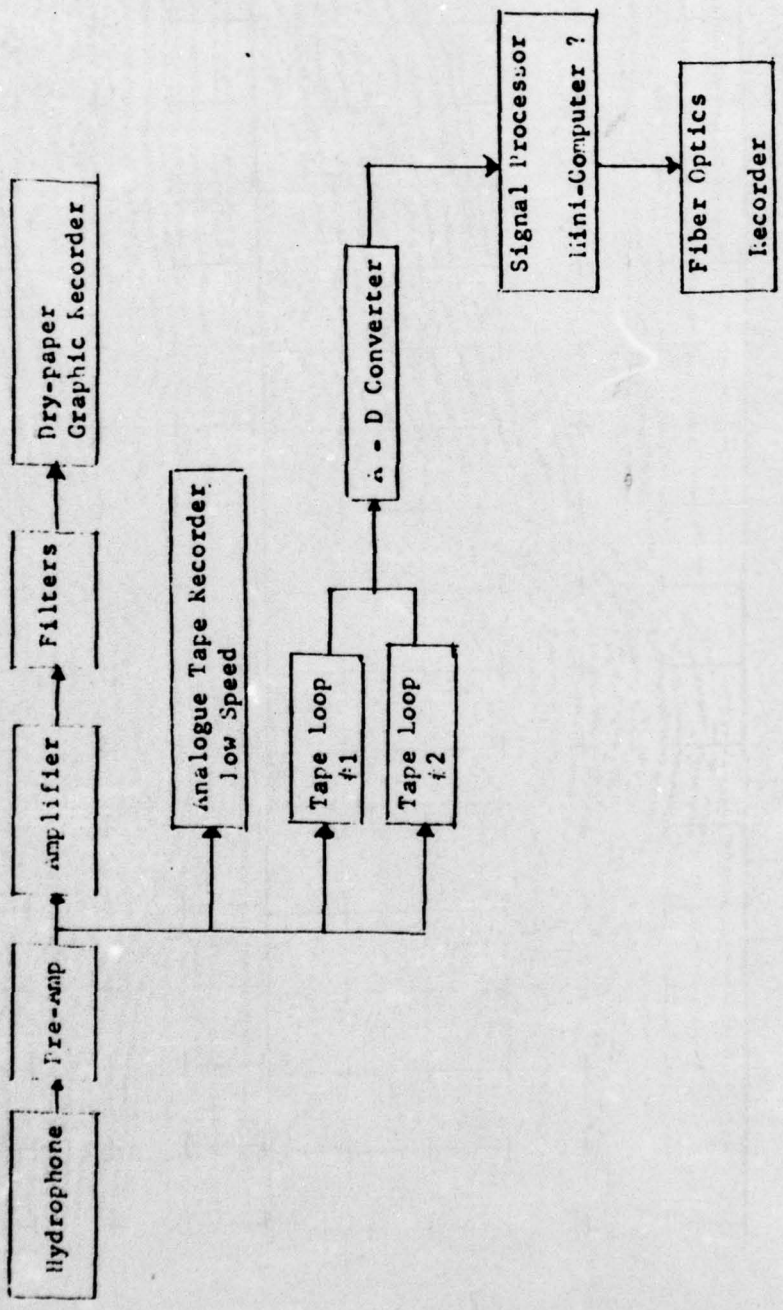
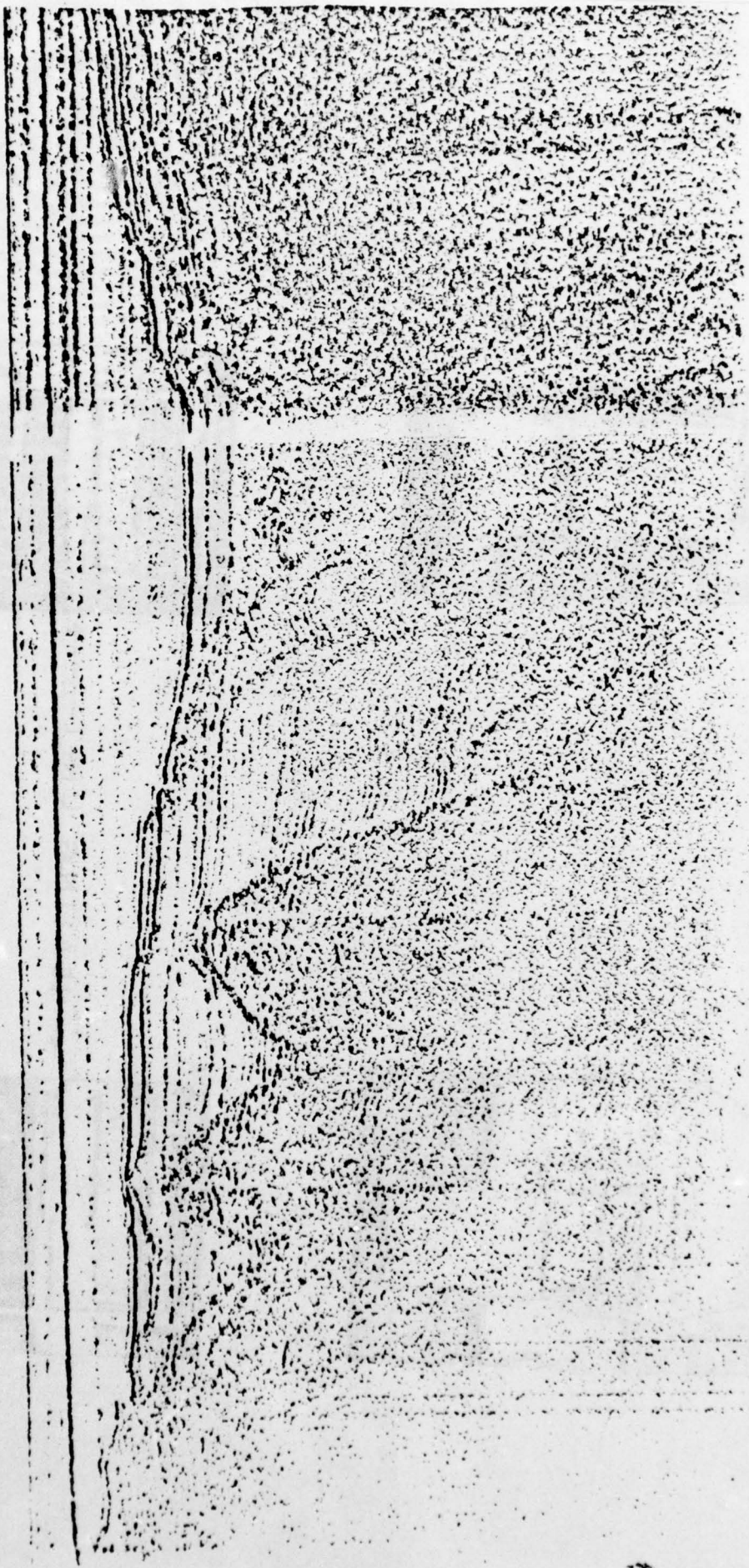


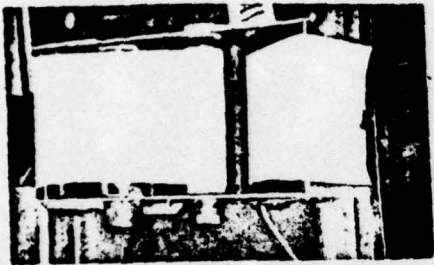
Figure 3



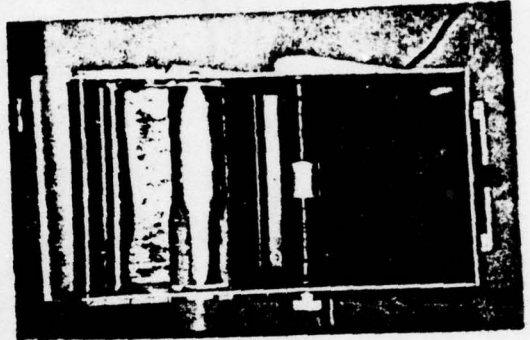
Run on Modified Honeywell 1218 Magazine - Type 777 Paper

Figure 4

BEST AVAILABLE COPY

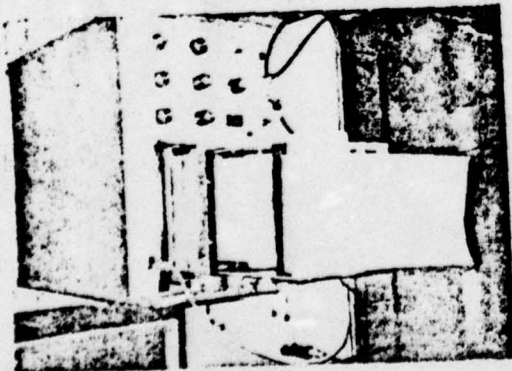


b



d

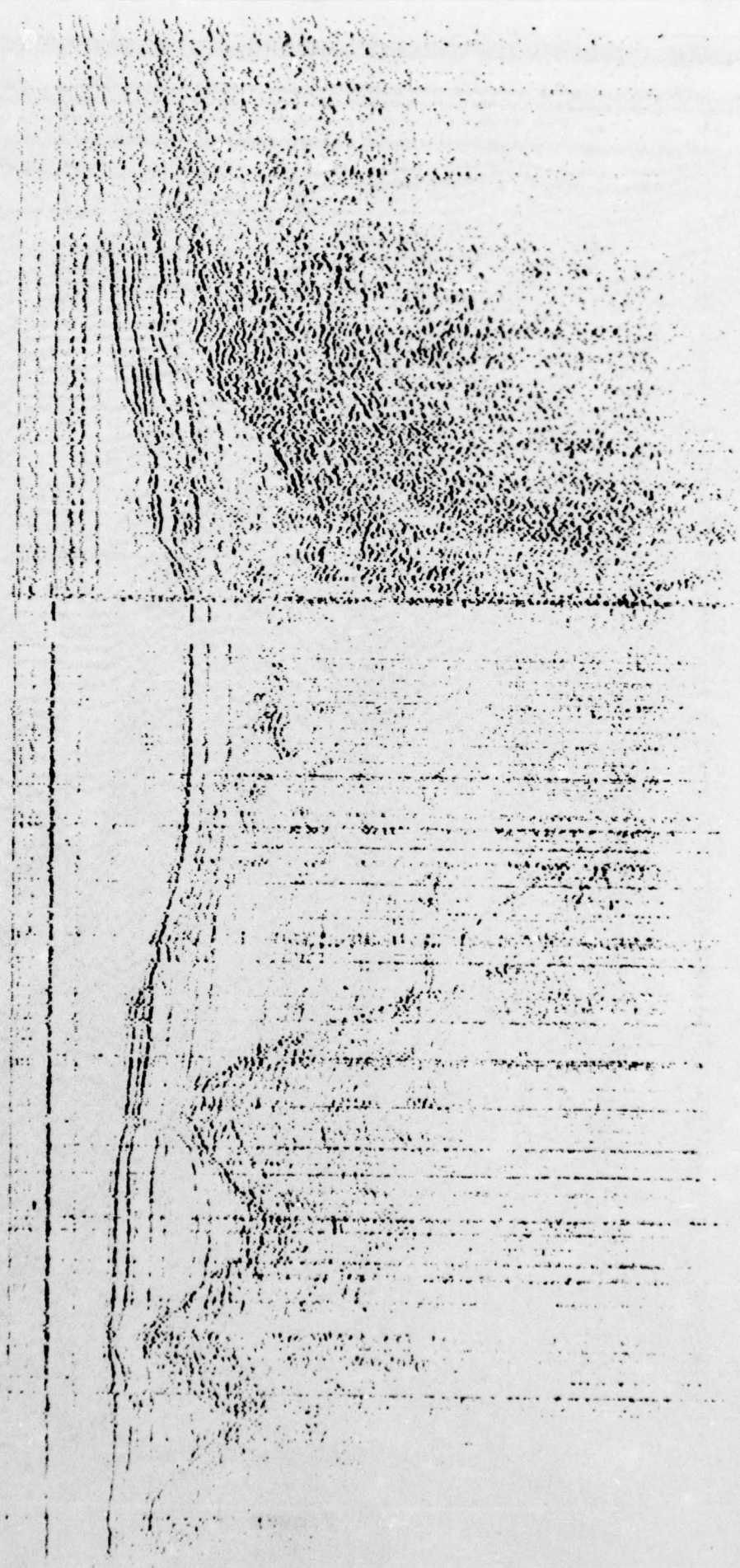
← HEATING UNIT →



e



c



Run on modified Honeywell 1218 magazine - Type 777 \approx mod 10/60

Figure 6

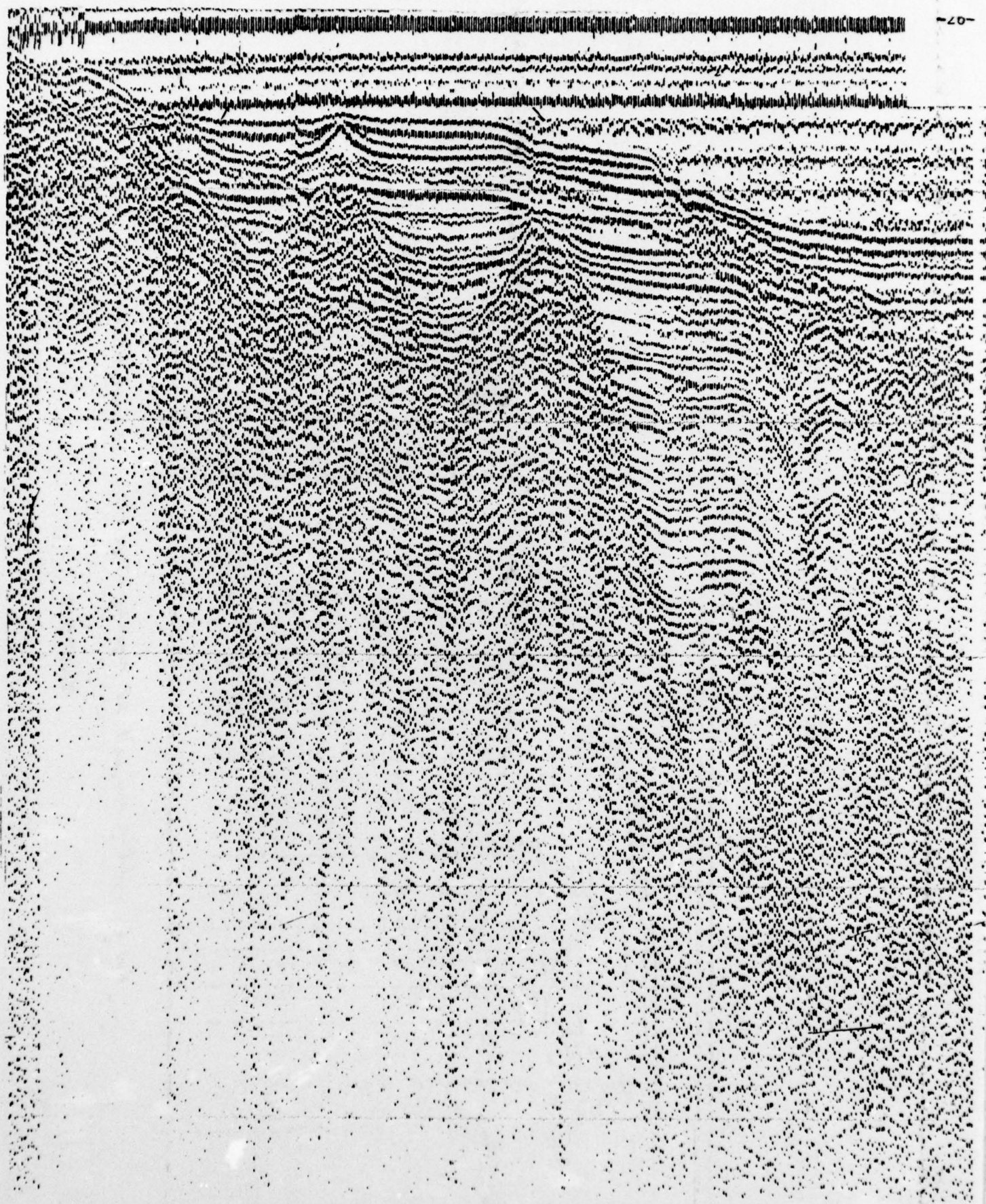
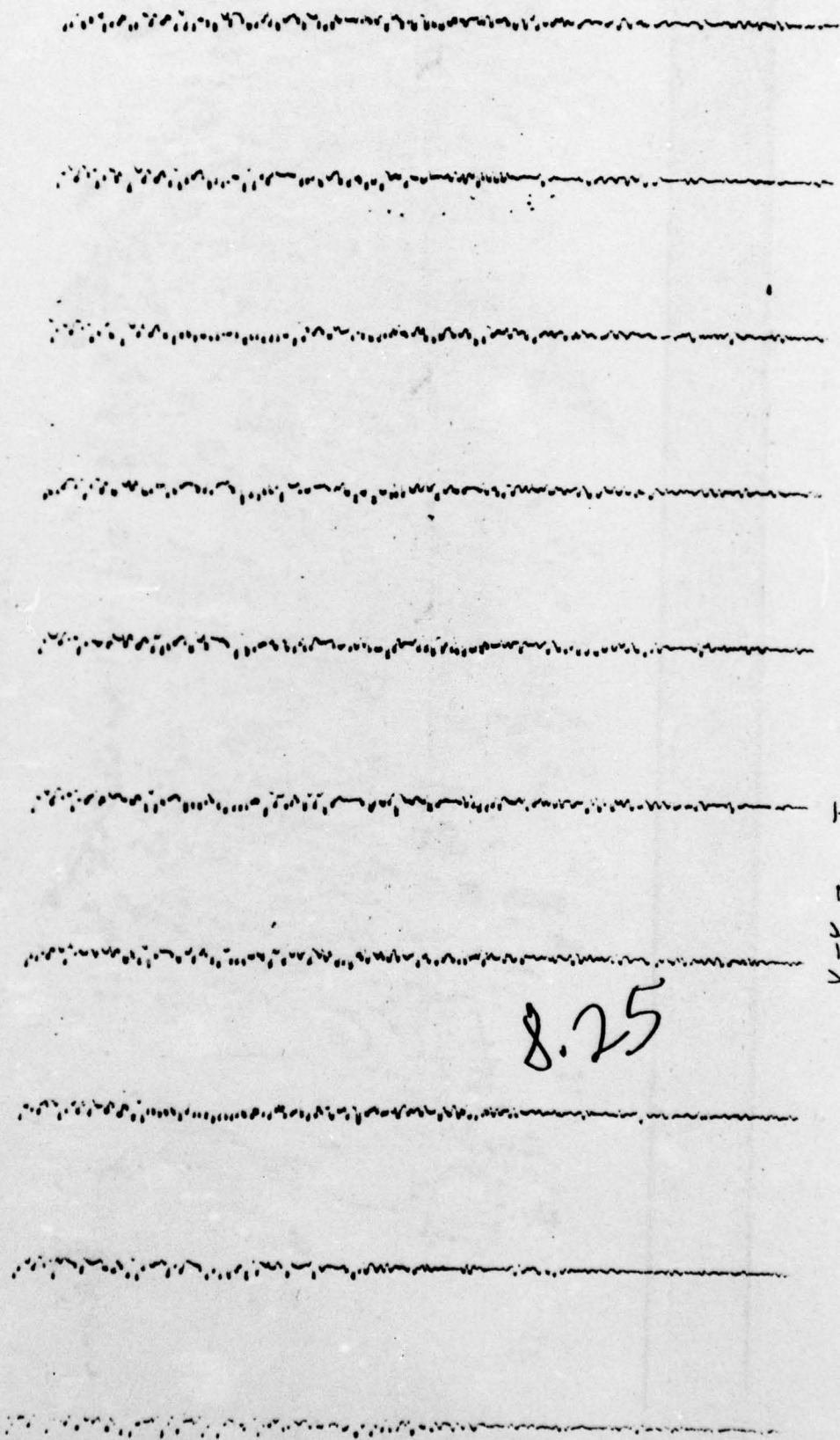


Figure 7



Thermal Imagery - Type 777
U.S. Processor - 2/14/73

Figure 8



2/12/73

X-Y-Z Type 777 1.33 cm/sec

8.25

Figure 9

3.2 cm/sec
8.5 intensity

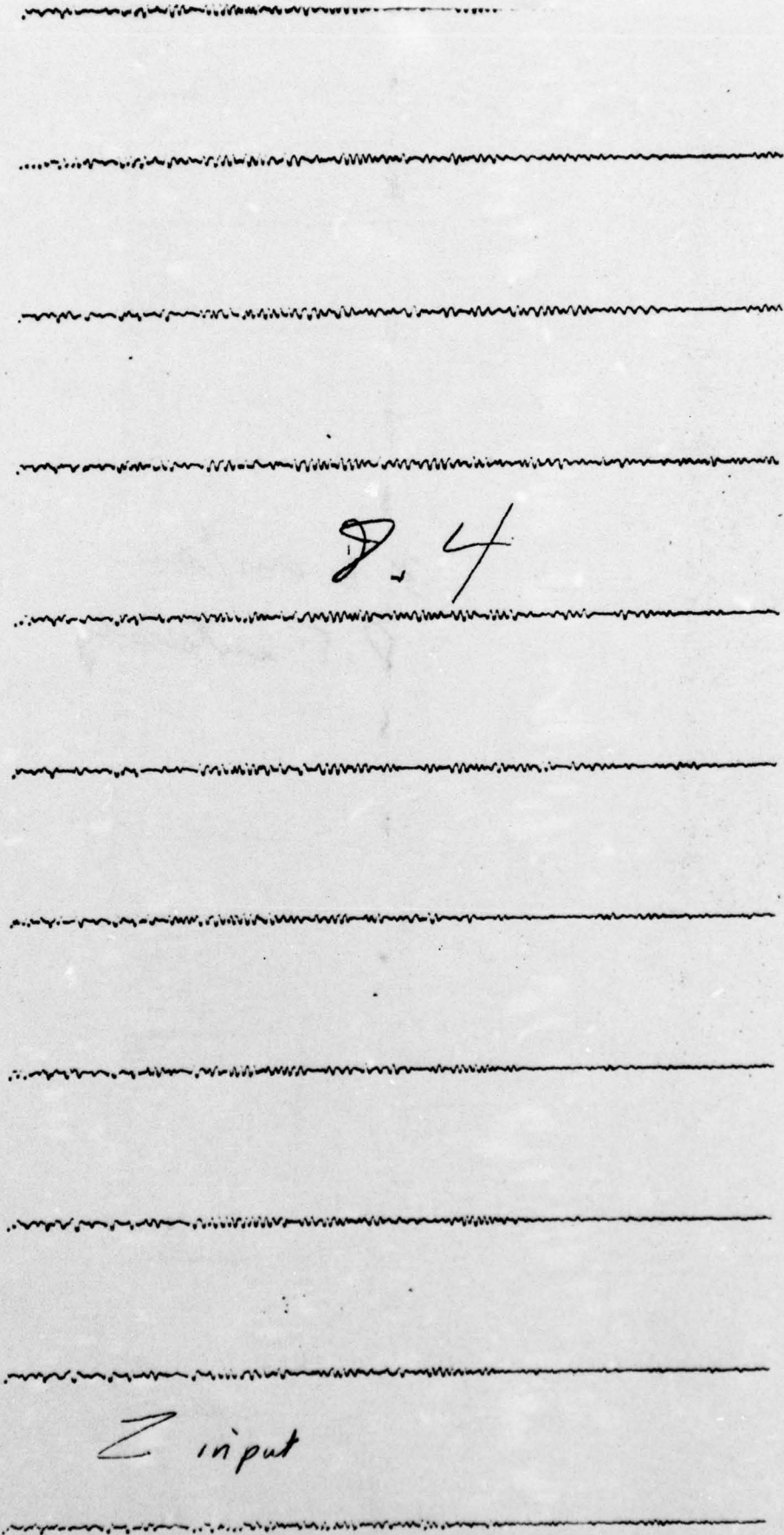
X-Y-Z

Type 777

3.2 cm/sec

2/12/73

Figure 10



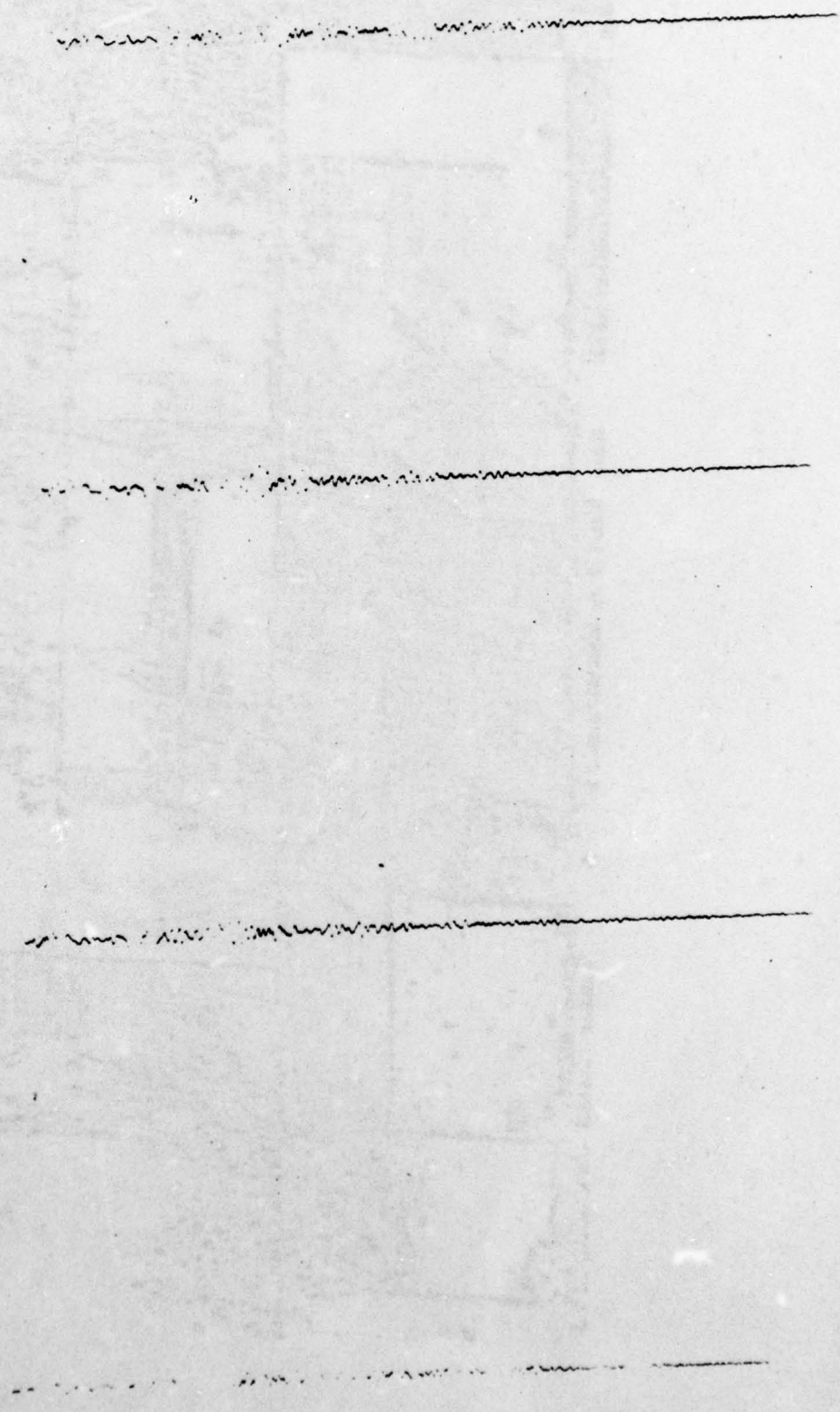
2/12/73

133 cm / 100

Exp.

X-1-E

Figure 11



Exp. 312 6/1/25

Figure 12

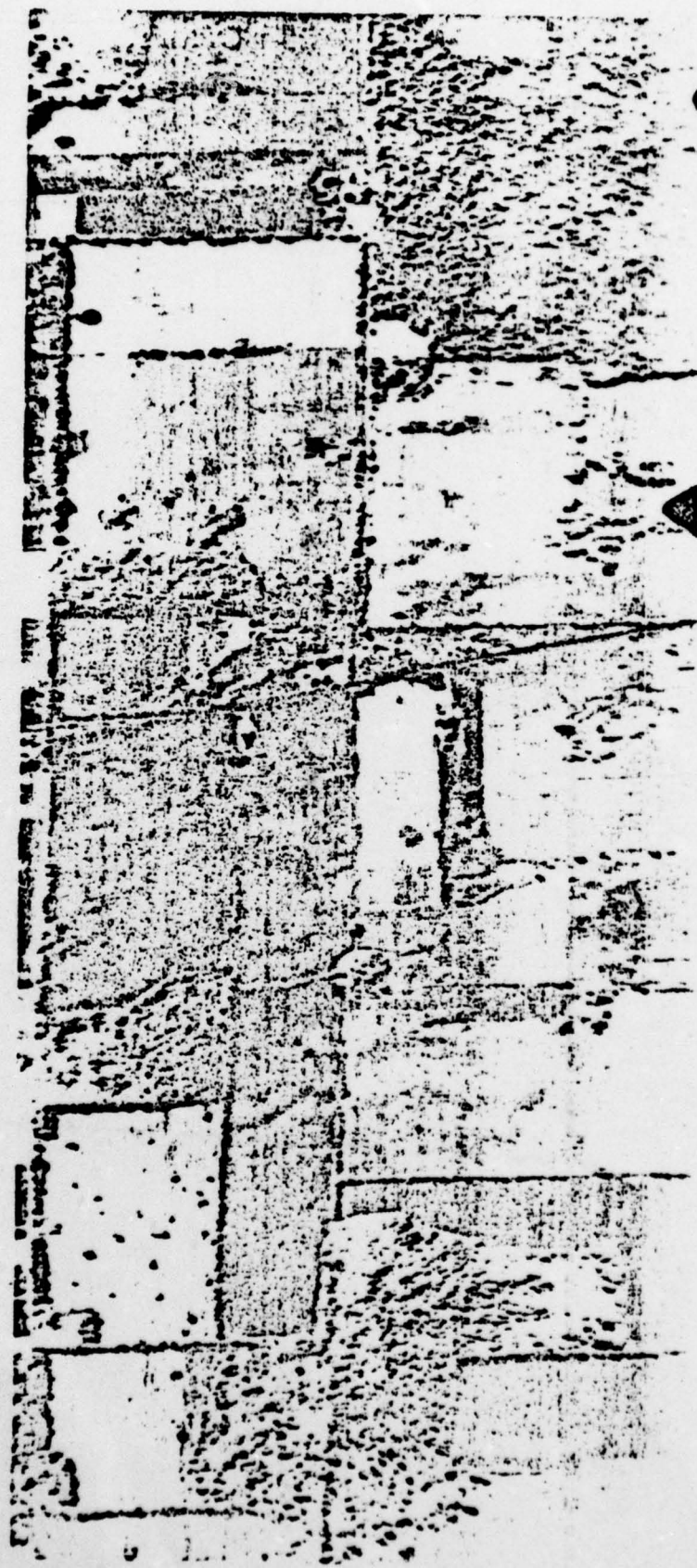
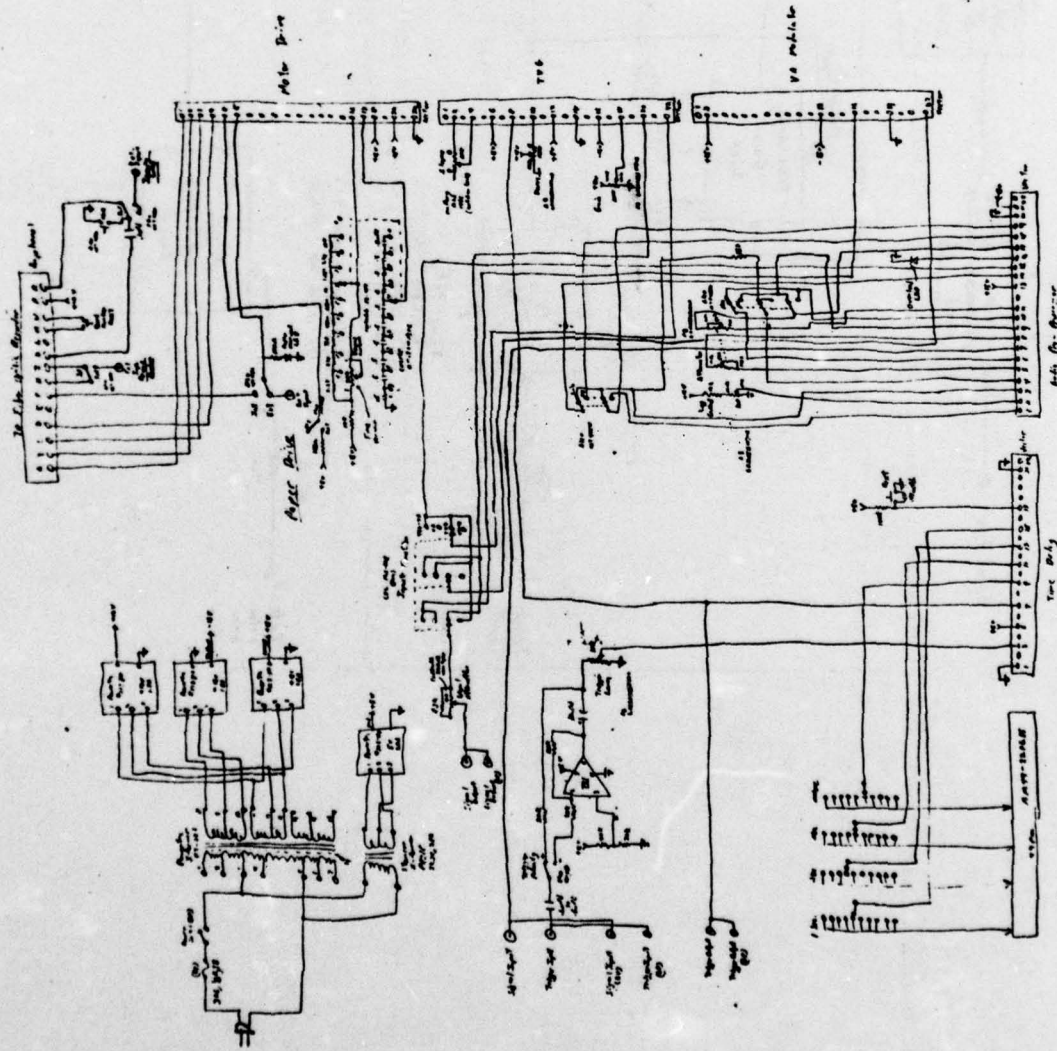
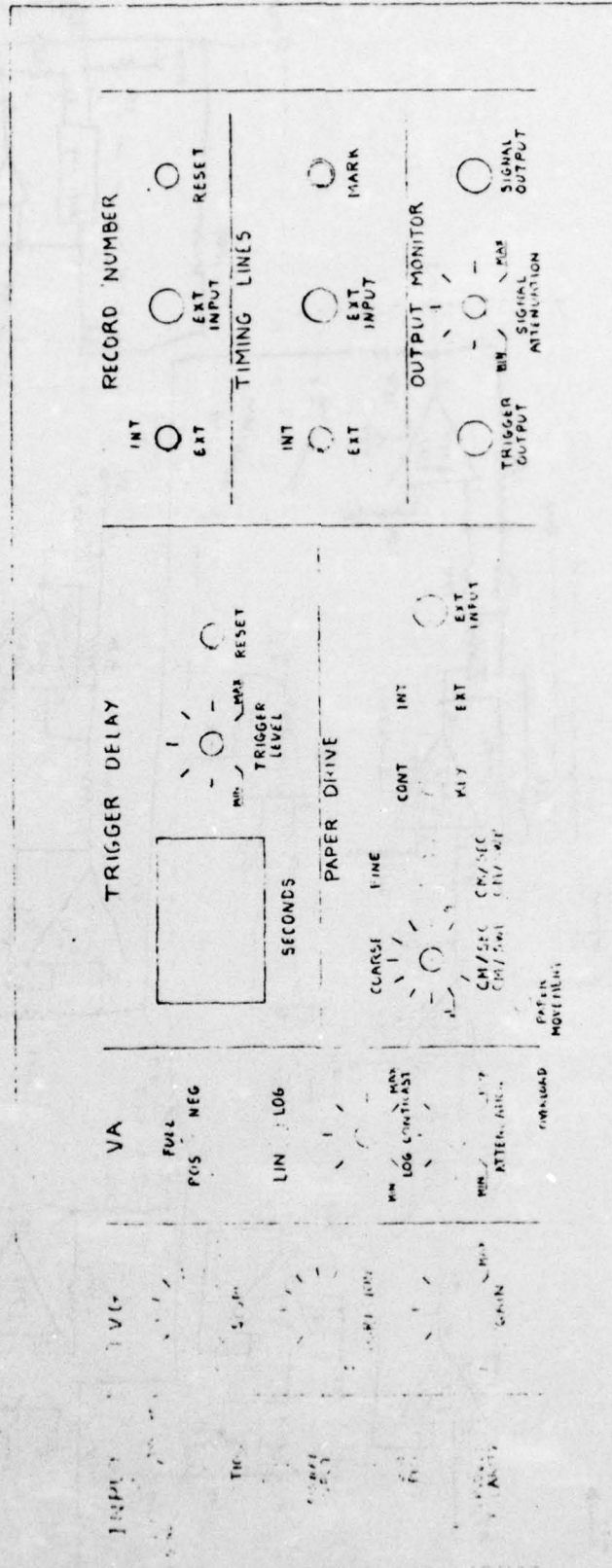


Figure 13



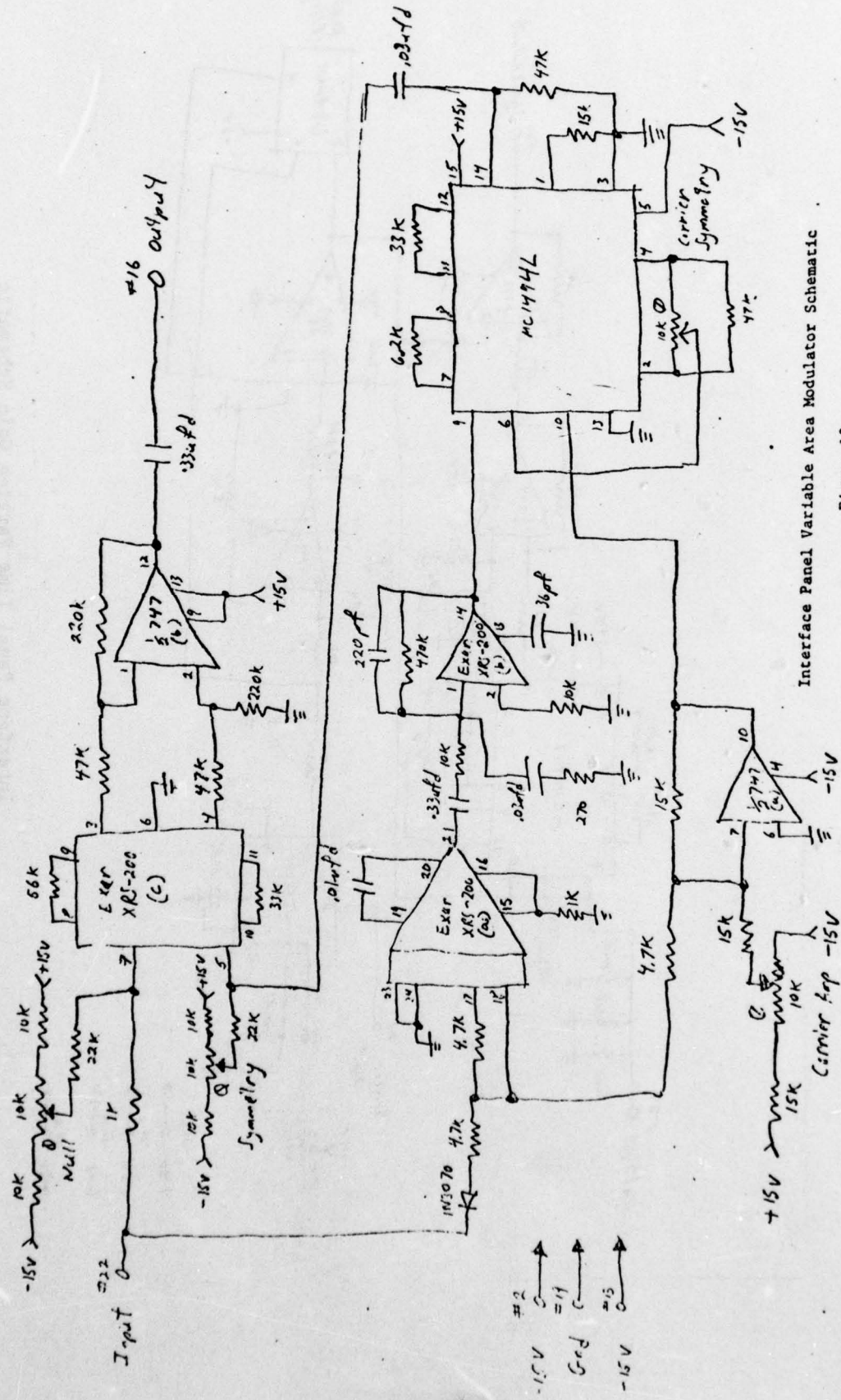
Schematic of IP Chassis

Figure 15



Interface Panel Front Panel Layout

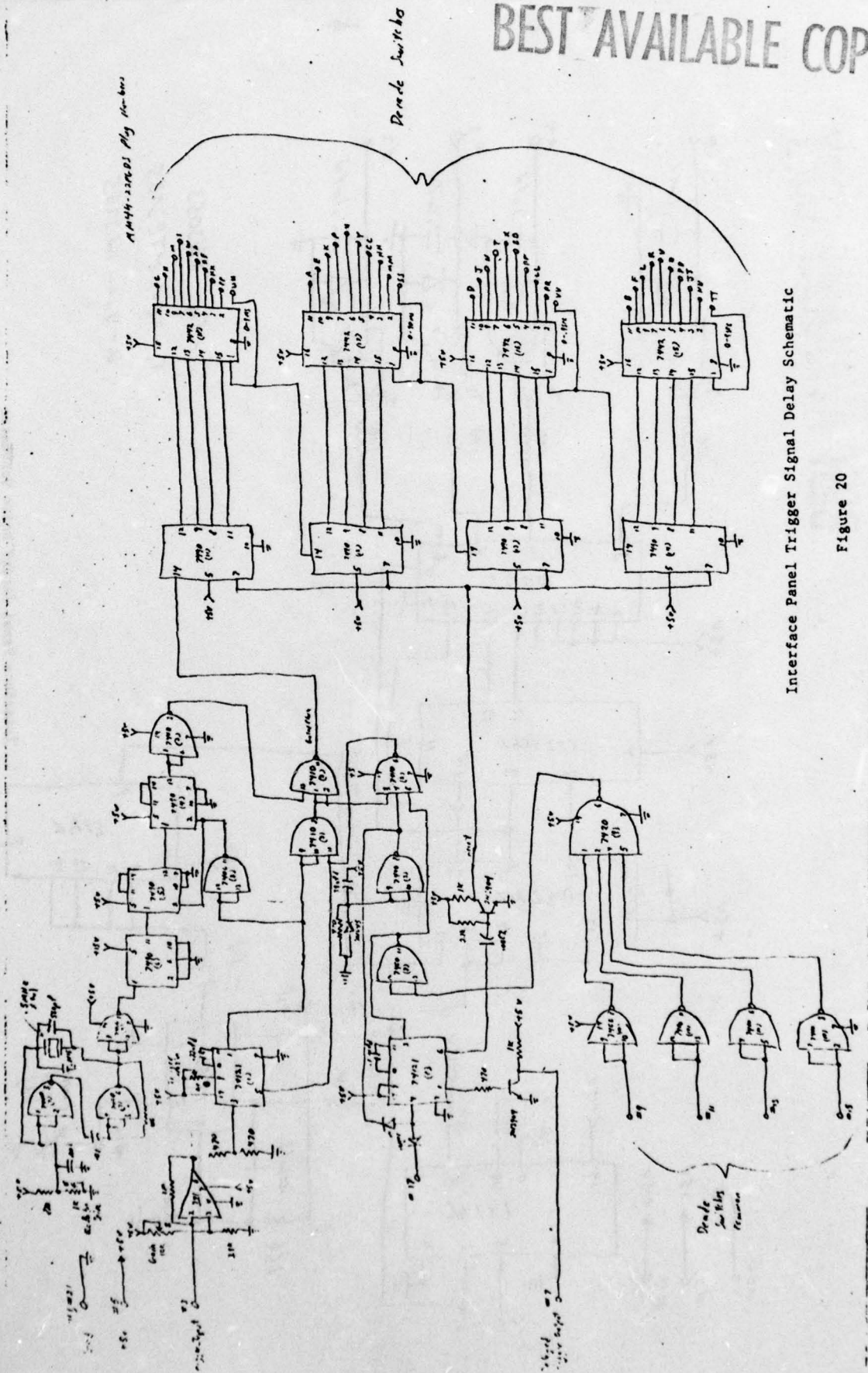
Figure 16



Interface Panel Variable Area Modulator Schematic

Figure 18

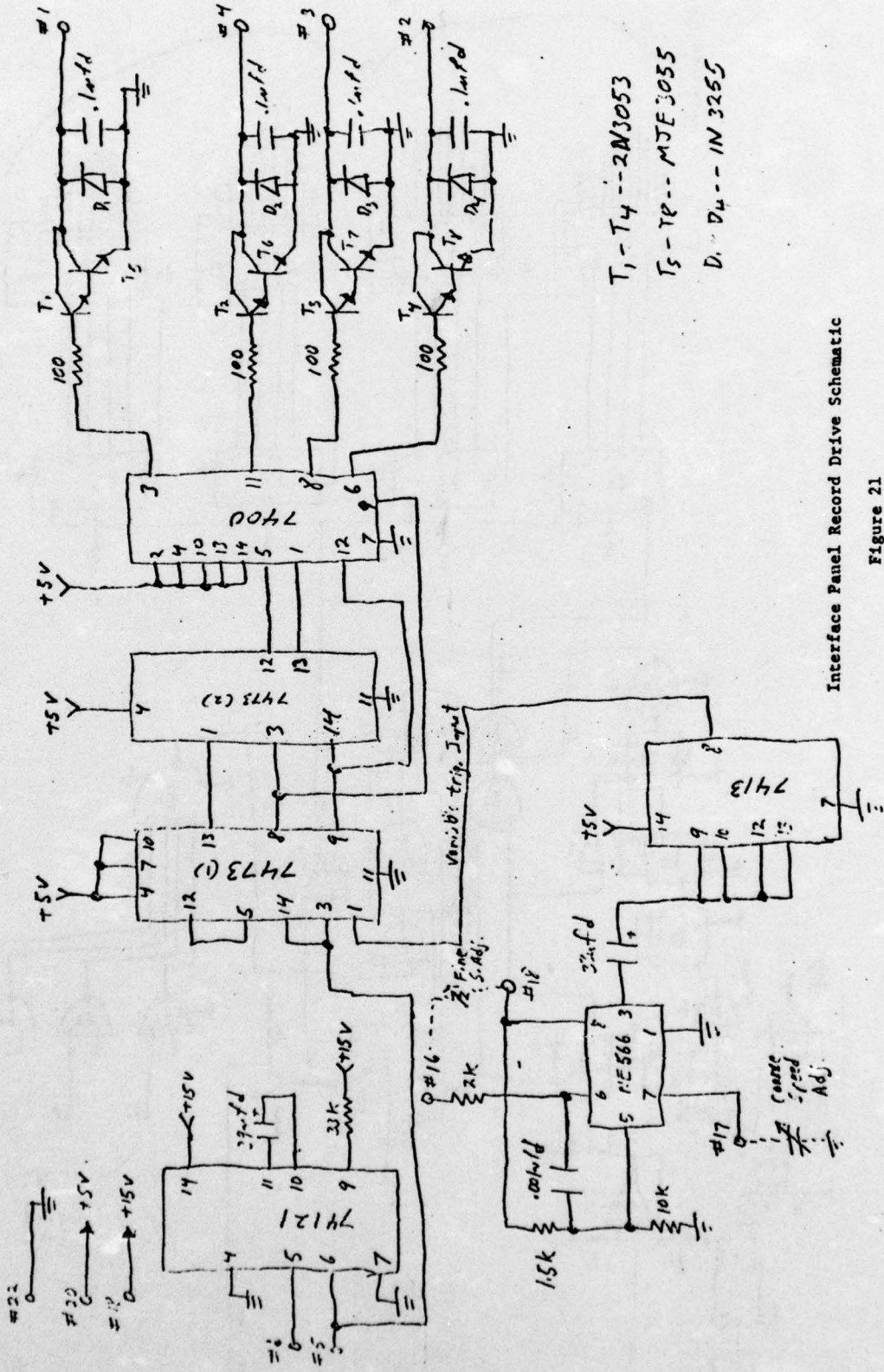
BEST AVAILABLE COPY



Interface Panel Trigger Signal Delay Schematic

Figure 20

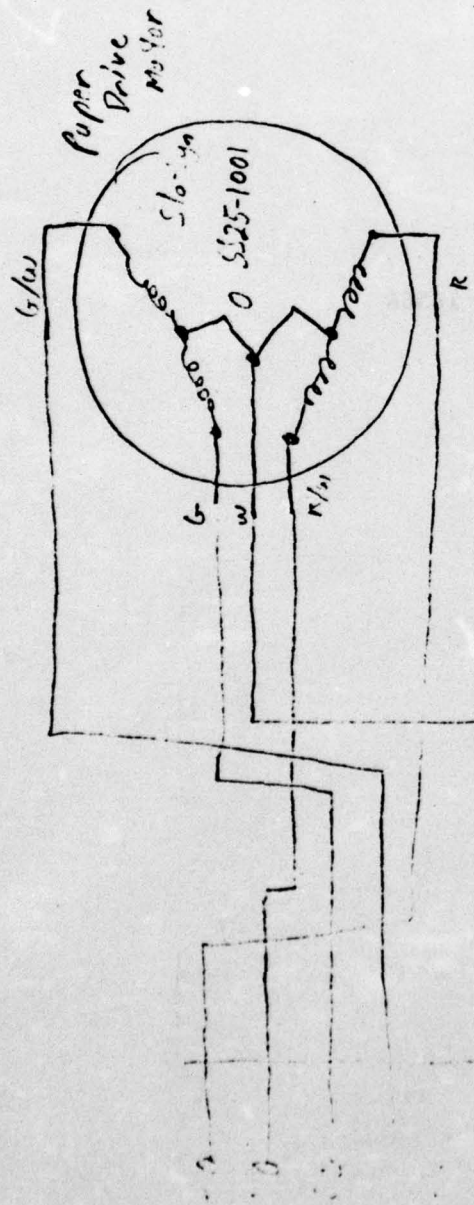
BEST AVAILABLE COPY



T₁ - T₄ -- 2N3053
 D₁ - D₄ -- MJE 3055
 D₁ - D₄ -- 1N 3255

Interface Panel Record Drive Schematic

Figure 21



- ▶ Blanketing (see Colpitt, A351 - See Fig. 7-11, Page 7-23/7-24
- ▶ Photoelectric Intensity, Part 2, A354 - See 14, 7-5, Page 7-11/7-12
- ▶ Power Photoelectric Intensity, Part 2, A354 - See Fig. 7-5 Page 7-11/7-12
- ▶ Reference Lines (Timing Lines) on 10, Pin 16, A4A7 - See Fig. 7-5, Page 7-11, Part 2 or A353
- ▶ Parallel Round Rod Colpitt, A355 - See Fig. 7-5, Page 7-11, 7-12
- ▶ Reference Lines, Intensity, Part 2, A353 - See Fig. 7-6 Page 7-13/7-14

Fiber-Optics Recorder Modifications Schematic

Figure 22

BEST AVAILABLE COPY

Appendix I

Technical Specifications

Honeywell Oscillographic Recorder Model 1856A

Honeywell Processor Model 1219

Oscillographic Recorders

MODEL 1856A

Operational Specifications

General

This instrument is designed, except as noted in the detailed specifications published herein, for operation in a laboratory-type environment. It can be used, with adequate environmental protection, in non-laboratory applications.

Recording System

Recording Media Kodak Linagraph
Direct Print Paper, wound emulsion out, on 3½-in. maximum diameter roll. (Spec. 2)

Standard weight, 6-inch width, 100 foot roll. P/N 16100338-001; thin base, 6-inch width, 200-foot roll. P/N 16757286-158.

Ektaline 12, RAR 2490, RAR 2491, du Pont RPR 4-inch maximum diameter roll may be used with the 1218A Magazine.

3M Brand 7770 Dry Silver Paper and 7859 Dry Silver Film on 4-inch max diameter rolls may be used with the 1219 Processor, emulsion out (Spec. 2)

Record Drive Speeds Servo-controlled
0.1 cm/sec to 50 cm/sec in 9 calibrated steps (1, 2, 5 sequence). Speed accuracy ±5 percent. Vernier control provides up to 2.5:1 decrease of speed between discrete steps. Pulley ratio change kit to provide a 5:1 increase in chart drive speeds (0.5 - 250 cm/sec) is optional.

Record Drive Modes:

Manual MOM (momentary on), stationary ON, and OFF.

Automatic Initiated with a sweep ending or sweep beginning (normal, free run or triggered mode) when the record overrun and drive switches are switched ON.

Record Overrun A control switch permits a programmed amount of paper travel in the automatic record drive mode. This control is adjustable from approximately 150 msec to 60 sec in 3 steps (controlled by record speed setting) to allow spacing between automatically recorded signals.

Recording Resolution Less than 0.005 inch spot size with 100 line pairs/inch.

Reference Lines

(Option) A transverse reference line may be recorded every centimeter along the record. This line includes horizontal reference markers spaced 1 cm apart. The transverse reference line may also be triggered by an external timing generator up to 250 lines per second. Spacing between 2 reference lines is 1 cm ±3 percent when triggering internally. For external trigger, triggering signal should be at least 10V pk-pk and within dc potential range of ±40V. The slowest allowable rise time of the trigger pulse is 1 msec.

Record Numbering

(Option) A 4-digit record number is recorded on the left margin of the record at the beginning of each manual start of the record drive. The number is automatically advanced one count after being recorded. (An internal link is provided to allow flash without advance when desired). The counter may be reset to zero or manually flashed and advanced by use of rear panel controls. Maximum cycle rate is 3/sec.

Vertical Deflection

(Option)

Automatic Sweep When vertical deflection amplifier is not used, the recording trace on the CRT is sweeping vertically at a maximum rate of 1 cm per 25 minutes.

Bandwidth Not more than 3 dB down at 75 kHz.

Sensitivity 1V pk-pk input for 1 cm ±5 percent deflection when the ATTN is set to CAL position. Vernier range: 1 to 10V/cm.

Input Impedance 1 megohm ±3 percent shunted by 35 pF maximum.

Maximum Input Signal ac peak + dc level not to exceed ±250V.

Gain Stability ±4 percent throughout operating temperature and line voltage ranges.

Vertical Input Connector on rear panel.

Horizontal Deflection Circuits (X-Axis)

Bandwidth dc to 18 kHz, -3 dB

External Sensitivity 0.5V per centimeter ±25 percent. Approximately -3V to +3V required for full scale sweep.

Sweep Range 2 μsec per centimeter to 1 second per centimeter in 18 calibrated steps of 1, 2, and 5. Continuously variable vernier control between steps decreases sweep speed at least 2.5 times. Sweep timing accuracy is ±4 percent, except on 2 μs/cm where it is ±7 percent. Uncalibrated sweep times up to 2.5 seconds per centimeter.

Input Impedance Greater than 100 kΩ

Linearity ±2.5 percent of full scale (measured by displacement from ideal)

External Horizontal Input Rating Maximum ac peak + dc level, ±25V.

Hold Off Time Time between free run sweeps. Sweep times from:
1 sec to 2 msec/cm ± 4 msec
1 msec to 2 μsec/cm ± 40 μsec.

Sweep Spacing A variable control adjusts spacing from approximately 40 μsec to approximately 6 sec in 3 steps (controlled by record speed setting) to prevent overlapping of recordings in free run and triggered modes.

Triggering

Sensitivity External dc to 1 MHz 2V pk-pk. Internal: dc to 75 kHz ½ cm pk-pk vertical display on FO-CRT, with Vertical Amplifier option installed.

Source Internal (vertical input), external (trigger input) ac or dc.

External Input Impedance Greater than 100 kΩ shunted by less than 350 pF.

External Input Level Maximum dc coupling, ac peak + dc level, ±80V ac coupling, ac peak + dc level maximum ±500V. On EXT DC, the unit will be triggerable with up to ±10V of dc superimposed on signal.

Trigger Modes Auto, Normal, Free Run

Controls Adjustable trigger level, and slope

AC Inputs External or internal
The low frequency ac coupled limit is 50 Hz.

Intensity Modulation Circuits (Z-Axis)

Bandwidth Down not more than 3 dB at 8.0 MHz.

Maximum Input Signal ac peak plus dc level not to exceed ±20V

Input Impedance Greater than 5 kΩ, resistance and less than 100 pF capacitance.

Input Sensitivity Z axis is blanked by an input variation of 2V to 5V, as determined by GAIN control. The variation may start from any input voltage within ±5V dc as determined by INPUT SUPPRESSION control. Polarity is set by POLARITY control such that with + set a positive change will blank the CRT, and vice versa. Controls located on top of recorder.

Blanking

Record Drive Unblanks the CRT for recording internal and external horizontal displays. May be overridden by auto blanking and Z axis signals.

Sweep Holdoff Will blank the CRT during retrace and rest time.

Oscillographic Recorders

MODEL 1856A

Auto Blanking Is used on EXT horizontal input only. The CRT will unblank if the input signal is greater than 10 Hz and 1 cm. This feature may be disabled by an internal jumper.

Output Circuitry

Gate Out During sweep blanking time TTL-compatible (high) pulses will be obtained on the GATE OUTPUT jack, with a resistive load of not less than 10 kΩ and a capacitive load of not more than 50 pF.

Numeric Printer

(Option)

Display Three sets of two numbers and an event mark appear on the right-hand side of the paper as it exits from the recorder. Each number is approximately 1/8 inch (3.18mm) high, and the entire display is approximately 1/2 inch (13mm) high. The entire display is approximately 5/16 inch (8mm) wide, and any signals which would otherwise appear in the space occupied by the numbers are blanked. An internal switch (on the printer card) allows proper operation regardless of beam scan direction. On reverse sweep, the numbers must be shifted inward slightly to insure sweep start. The highest number combination that may be recorded is 39-79-79.

Electrical The sequence of printing a timing mark and numbers is initiated by the print command signal going high (+2.4V min) and remaining high for a minimum of 200 nanoseconds. All numeric inputs (coded in 20-line BCD) are compatible with TTL voltage levels: Binary One is +2.4V dc min, 5.0V dc max; Binary Zero is 0V min, +0.4V max. Inputs must be stable when the print command goes high and remain stable for 200 nanoseconds. A mating input connector (Amphenol 57-30360) P/N 16750110-015, is furnished.

Restrictions The numeric printer is used only for line scan recording. Sweep speed/repetition rate and paper speed must be adjusted so that successive scans of the CRT beam produce overlapping (or touching) lines. The front panel intensity control must be adjusted so that the blanking amplifier can control the beam intensity. No restriction is placed on the top-panel controls (Polarity, Gain, Input Suppression). The Numeric Printer may not function on sweep speeds faster than 20 micro-seconds/cm because of digital logic reset times.

Environmental Specifications

Ambient Temperature Operating 0 to +50°C (32 to 122°F). Non-Operating: -55 to +60°C (-67 to 140°F.)

Humidity 5 to 95 percent, Relative (non-condensing)

Altitude Operating: Up to 10,000 feet above sea level. Non-Operating: Up to 50,000 feet above sea level.

Recovery Time From non-operating to operating environmental conditions - 4 hours maximum.

Power Requirements

Power 107-127V, 48 to 62 Hz; switch selectable 214-254V, 48 to 62 Hz; 350W max. Also available for 107-127V, 400 Hz. (Internal tap changes for 98-116V, or 196-232V, 45-62 Hz.)

Reliability

The Honeywell Model 1856A has been designed to provide the maximum in reliability and minimum maintenance. The design program included Quality Assurance design review and a mean-time-between-failure (MTBF) prediction.

To aid the user in determining maintenance requirements, the estimated MTBF of any 1856A system configuration can be determined from the table below.

This prediction was performed using MIL-HDBK-217A failure rates (paragraph 7.0) and the K-Factors for GROUND environment. A detailed parts application review (a review to ensure that all parts are correctly applied and that parts are not overstressed by voltage, current, power or temperature) was performed.

Based on the fact that all the parts are correctly applied and are not overstressed, the prediction was performed in accordance with MIL-HDBK-217A, para. 4.5, utilizing specific parts count on part types

operating at an ambient temperature of 50 degrees C. The stress ratios selected were those that are typical of Honeywell's derating practice.

The estimated mean time between failure assumes an exponential distribution. The failure rate allocations for the specific system elements are summarized in the table.

Component	N Units	λ F/10 ⁶ hrs.	Nλ F/10 ⁶ hrs.
Basic Unit	-----	260.02	-----
Latensifier	-----	1.53	-----
Modification Kit Record No.	-----	3.57	-----
Modification Kit - Vertical Deflection Amp.	-----	8.62	-----
Modification Kit - Reference Line System	-----	4.45	-----
Total (ΣNλ)	-----	-----	-----
MTBF = 1 / Nλ	-----	-----	-----
= 1 / ----- x 10 ⁶	-----	-----	-----
= ----- hrs	-----	-----	-----

Packaging Specifications

Weight Less than 80 pounds (36.4 kg)

Dimensions

Bench: 11 1/8 inches (28.3cm) high, 16 3/4 inches (42.5cm) wide, 21 inches (53.3cm) deep max. Rack mounting: 10 1/2 inches (26.7cm) high, 19 inches (48.3cm) wide, 21 inches (53.3cm) deep

Ordering Information

Specify Honeywell Model 1856A Fiber Optic Line Scan Recorder

See chart below for exact model number selection.

Selection of Features to be Installed	BASIC MODEL NO.	RECORD NO.	VERTICAL AMP	REFERENCE LINES	POWER SOURCE
	1856A-H				
Record Numbering		N			
Vertical Amp			V		
Reference Lines				R	
50/60 Hz Power					6
400 Hz Power					4

(Basic recorder includes one roll of paper, two manuals, power cord and fuses)

Accessories

	Part Number
Rack Mounting Kit	16773691-001
Latensifier	16761929-007
Service Kit	16774896-001
1218A Film Magazine with 1856A Adapter	16771238-001
1219 Processor with 1856A Adapter	16791151-001
Instruction Manual, 1856A	16779054-001
Instruction Manual, 1218A/1219	16791152-001
Rack Mount Take-up Unit	16795587-003
Speed Change Kit	16774323-001

Special Options

Analog Multiplex Card Modification	SS2815
Numeric Printer Module	16792252-001

Operation

To use the Model 1219 Processor, simply load the processor with either Dry Silver paper or film and mount on the 1806A or 1856A Visi-corder. The light-tight unit can be directly attached to the 1806A. An adapter is required to attach the processor to the 1856/1856A. A darkroom or loading bag will be required to load the processor. The processor is designed for easy loading, simply remove the top and supply covers, insert the supply spindle into the paper or film roll, install the supply spindle, pull the paper across the pressure pads and platens, reinstall covers. No difficult threading required. The loaded light-tight processor is then installed and the power cord connected to facility power.

Controls

1. Heaters - Allows selection of either one or both heaters as required by the RECORD SPEED selection on the 1806A and 1856/1856A. NOTE: Power is removed from the heaters when the top cover is removed.
2. Temperature - Multiturn, calibrated dial with locking knob sets the temperature of the heated platen(s). Required setting is determined by the RECORD SPEED selection on the 1806A and 1856/1856A. The higher the record speed, the more temperature required to heat-develop the media.
3. Drive - Supplies power to the processor and drive motor. Selection of either High or Low is as required by the setting of the RECORD SPEED selection on the 1806A or 1856/1856A.

Indicators

1. Power - Indicates power ON/OFF to the processor.
2. Heater - Glows when heater is on full duty cycle, cycles with heater when temperature setting is reached.

stability normally associated with wet process, photosensitive paper and film, plus the convenience of dry process. Stored under prescribed conditions of temperature and humidity, the paper and film have a shelf-life of 6 months or longer.

The processor accepts media rolls up to 4 inches in diameter and 6 inches in width. The length of the recording media depends upon thickness and is limited by the 4-inch maximum roll diameter, typically 200 feet.

The Dry Silver paper or film is in intimate contact with the faceplate of the FO-CRT where it is exposed, then passes over heated platens for development of the latent image. Two heated platens are utilized, one platen for record speeds below .1 cm/sec., both platens above .1 cm/sec.

All operator controls are located on the front panel. The 1219 Processor has special safety interlocks built in. The power to the heated platens is removed when the top cover is removed, exposing the platens, and all power is removed when the unit is not installed on an 1806A, 1856 or 1856A recorder.

Applications

The addition of the 1219 Processor to the series 1806A Recording Oscilloscope and 1856/1856A Line Scan Recorders provides unique solutions to the following special requirements:

- When higher contrast black-on-white records are required than obtainable with Direct Print recording materials.
- When higher net densities are required.
- When wider range of gray scale is required.
- When the final record must be of high quality, dry-processed and/or reproducible.
- When the final record must be able to be analyzed immediately.

10/15/74

-47-

PRODUCT INFORMATION

Oscillograph Recorder
Model 1219 Processor

Product Information

Increases versatility of Honeywell Models 1806A, 1856 and 1856A Visicorders by providing black-on-white and a wider range of gray scale recordings.

Outstanding Features

- Black-on-White Recordings
- Gray Scale Recordings
- Dry Process Developing
- Processes Paper and Film
- Easy Loading, Light-tight
- Recording Media Roll Diameters up to 4 Inches
- Light Weight
- Extends Versatility of 1806A, 1856 and 1856A.

Product Description

Honeywell's new Model 1219 Processor is an accessory for the series 1806A Recording Oscilloscope and 1856A Line Scan Recorders, which use photosensitive, heat-developing paper and film to record data displayed on the fiber optic CRT. The 1219 Processor is especially advantageous when off-line, wet chemical processing is not available or inconvenient to use in such areas as aircraft installations for seismic or oceanography displays and remote instrumentation vans for geophysical logging.

The 1219 Processor is designed to use 3M brand type 7770 Dry Silver paper and type 7859 Dry Silver film. The type 7770 paper and type 7859 film provide both high contrast (black-on-white) or gray scale recordings. Dry Silver paper and film offer the

Operational Specifications

Recording Media: 3M brand type 7770 Dry Silver paper or type 7859 Dry Silver film, specification 1 (emulsion in) or specification 2 (emulsion out) on a 4-inch maximum diameter roll. The 7770 Dry Silver paper and 7859 Dry Silver film (splice-free) are available from:

3M Company
3M Center
Building 220-9E
St. Paul, Minnesota 55101.

Writing Speed: Usable to 20,000 ips with 7770 paper. Recording medium limited.

Record Speed: The RECORD SPEED selection on the 1806A and 1856/1856A determines the 1219 Processor speed. The Drive selection on the processor must be set to the selected speed range. For optimum results, the normal processing speed is from .015 cm/sec. to 5.0 cm/sec. Maximum recording speed is 12.5 cm/sec. for 7770 paper and 5.0 cm/sec. for 7859 film.

Accuracy: The record speed accuracy of the total recording system (1219 Processor and 1806A or 1856/1856A) is better than +10%.

Loading: The supply chamber ^{must be} ~~can be~~ loaded using a loading bag or under darkroom conditions.

Recording Medium Supply Indicator: Indicates percent of 4-inch diameter roll remaining in supply chamber.

Trace Quality: Trace quality is dependent upon the temperature setting of the 1219 Processor; Intensity Control on the 1856/1856A; the Focus, Astigmatism and Intensity Control settings on the 1806A, and the condition of Dry Silver paper and film. The technical manual, supplied with each processor, gives approximate temperature settings for various record speeds. Desired quality

is best obtained through the trial process by the operator. A viewing window is provided so that the operator may see the results of any adjustments before the medium exits from the processor.

Warmup Time: 20 minutes from initial turn-on.

Delay Between Printing and Viewing: 13 inches.

Environmental Specifications (Excluding Recording Medium)

Ambient Temperature: Operating: 0 to +40° C (32 to 104° F). For best results with the medium, the recommended operating temperature is 15 to 35° C (59 to 95° F).

Non-operating: -20 to +65° C (-40 to +149° F).

Humidity: 0 to 95% relative (non-condensing). Recommended - 0% to 50%.

Altitude: Operating: To 10,000 feet above sea level.

Non-operating: To 50,000 feet above sea level.

Power Requirements: 107-127V, 48 to 62 Hz, 650 watts maximum. An external step-down transformer (not supplied) is required for 214-254V, 48 to 62 Hz operation. Not operable on 400 Hz.

Packaging Specifications

Net Weight: Less than 18 lbs. ^{add Kg} (excluding recording medium).

Shipping Weight: Less than 36 lbs. ^{add Kg}

Dimensions: 8" wide, 9½" high, 16" deep maximum
(20.4 cm wide, 23 cm high, 40 cm deep).

Ordering Information

<u>Specify:</u>	<u>Part Number</u>
Model 1219 Processor	
For Model 1806A	16791151-002
For Models 1856/1856A (Includes Adapter Kit for 1856/1856A)	16791151-001
Adapter Kit (1856 or 1856A)	16791181-001

Ordering Information (cont'd.)

	<u>Part Number</u>
Instruction Manual, 1219	16791152-001
Step-down Transformer, 750 watts (for 214-254V operation)	16791204-001

Appendix II
The Development and Evaluation
of a New Marine Seismic Energy Source:
The HP Water Gun

THE DEVELOPMENT AND EVALUATION
OF A NEW MARINE SEISMIC ENERGY SOURCE:
THE HP WATER GUN

BY

BILL L. JAWORSKI

A thesis submitted in partial fulfillment of the
requirements for the degree of

MASTER OF SCIENCE

GEOLOGICAL SCIENCES

at the

UNIVERSITY OF WISCONSIN-MILWAUKEE

April, 1975

Examining Committee:
Dr. R.J. Wold, Chairman
Dr. R.W. Taylor
Dr. R.G. Pirie

ABSTRACT

The implosive generation of seismic energy offers inherent advantages over explosive techniques. Explosive generation of seismic energy results in considerable energy remaining in the bubble/afterflow system after initial signal generation. Oscillations of the bubble result in secondary events of the radiated acoustic signal. Attenuation of the secondary effects or bubble pulse requires large arrays of energy sources or significant loss in radiated acoustic energy.

Implosive generation of seismic energy uses the collapse of a vacuum volume to generate a broad band, high amplitude acoustic pulse. The transfer of energy from the source to the marine environment must be a relatively long-term process relative to explosive methods. A long-term transfer of energy allows the use of mechanisms not practical in explosive techniques.

The system developed at the University of Wisconsin-Milwaukee uses the implosive generation of seismic energy coupled with a highly efficient restoring mechanism. Dynamic characteristics inherent in the vacuum volume generation allow the use of a hydraulic/pneumatic restoring mechanism. The use of a hydraulic system as the prime energy transfer mechanism coupled with a low compression, high pressure pneumatic system results in an extremely efficient system.

ACKNOWLEDGMENTS

I would like to thank Dr. R.J. Wold, my advisor at the University of Wisconsin-Milwaukee, for his guidance and perspective throughout the preparation of this thesis; Clarence Huebschman and the Center for Great Lakes Studies, for turning my drawings into metal; the Great Lakes Research Facility, for its assistance; Sue Lukowski, for typing the manuscript; the United States Geological Survey, Office of Marine Geology, Woods Hole, Massachusetts, for assistance in testing; and Dick Edwards, of Woods Hole Oceanographic Institution, for his help and overview.

This research was supported by the Office of Naval Research, under contract number N00014-67-0128-0016, for marine geophysical instrumentation.

TABLE OF CONTENTS

	Page
Abstract	ii
Acknowledgments	iii
List of Figures	v
Introduction	1
Signature	3
Efficiency	22
Current Energy Sources	24
Air Guns	24
Vaporchoc*	27
Hydro-Sein*	29
Sodera-Water Guns	29
The HP System	32
Description and operation	33
Field Tests	45
Comparison of Prototype and New Design	50
Conclusions	55
Suggestions for Further Research	56
References Cited	57
Appendix	58

*Registered Trademarks Listed in Appendix

LIST OF FIGURES

Figure	Page
1. The idealized near-field signature of a typical explosive energy source in the time and frequency domain	5
2. The idealized near-field signature of an isotropic implosion in the time and frequency domain	6
3. The idealized far-field signature of a typical explosive energy source in the time and frequency domain	7
4. The idealized far-field signature of an isotropic implosion in the time and frequency domain	8
5. Effects of reducing the passband of an implosive far-field signature	11
6. The effects of reducing the passband on the far-field signature of an explosive energy source	12
7. The bubble cycle of a compressed gas explosive seismic energy source	17
8. The far-field signature of the Vaporchoc*	28
9. Comparison of the db. spectrum of a 16 unit air gun array and the Casios Simplon Water Gun*	31
10. Simplified cross section of the HP water gun	37
11. The operational cycle of the HP water gun	39
12. The schematic of the hydraulic and high pressure air systems of the HP water gun	40
13. The schematic of the electrical control and monitoring system of the HP water gun	41
14. Detail cross section to the face seal between the air-water piston and the valve housing	42
15. Photograph of the HP water gun	43
16. Photograph of the HP system	44

*Registered Trademarks Listed in Appendix

Figure		Page
17.	Schematic of the hydrophone/water gun during testing	46
18.	Schematic of the electronic equipment used during testing	47
19.	The far-field signature of the HP water gun fired at 650 psi	48
20.	Cross section of the new design	51

INTRODUCTION

1

Most marine seismic energy sources have traditionally generated acoustic signals which exhibited unwanted secondary events. Although some systems have succeeded in significantly reducing the magnitude of these secondary events, they still require bulky, inefficient and often unreliable components. The limitations imposed by the physical size of onboard supply units have become increasingly serious as larger and more powerful systems are deployed to supply greater penetration and resolution.

The prototype system developed at the University of Wisconsin-Milwaukee, the Hydraulic-Pneumatic Water Gun or HP system, succeeds in greatly reducing system weight while generating a signal essentially free of secondary events. A reduction in total system weight of approximately 60 per cent for the prototype HP system relative to an air gun system of similar seismic power output has been attained. An overall reduction of system weight of 75 per cent could be achieved if a large system were constructed. The reduction in system weight is primarily due to the use of a hydraulic system to restore the water gun.

The HP gun uses the collapse of a vacuum bubble to generate the acoustic pulse. The implosive collapse of a vacuum volume results in, essentially, a single impulsive acoustic pulse without any major secondary or bubble events. Vacuum volume generation is achieved by the rapid ejection of a volume of sea water from the muzzle of the source. The ejected water slug draws a vacuum behind it which subsequently collapses generating the acoustic signal.

The incorporation of a hydraulic recycling mechanism coupled with the implosive generation of the broad band acoustic signal allows the efficient gathering of high resolution data while still obtaining deep penetration. Weight reduction allows a survey to be conducted from a smaller vessel than would otherwise be possible.

SIGNATURE

The evaluation of the effectiveness of a seismic energy source ultimately rests on the quality of the data capable of being obtained with it. Reflection seismograms record results of the convolution of the impulse response of the subsurface with the radiated pulse when it enters the sea bottom. Modification of the impulse response of the earth is clearly neither possible or desirable. Improving the quality of raw data, therefore, becomes a function of improving the quality of the radiated acoustic pulse.

The signature of a marine seismic energy source is the graph of the pressure versus time of the generated acoustic pulse. Two different types of signatures are used. The far-field signature is the graph of the generated acoustic pulse as it appears as it enters the sea floor at a great distance from the source. Generally, the far-field signature implies that the longest wavelength of interest in the acoustic signal is much shorter than the source-hydrophone distance. Boundary effects, namely, the reflection of the original signal off the air/water interface, or ghost are included on the far-field signature.

The near-field signature is the graph of the acoustic signal generated by the seismic energy source as it appears a short distance from the source. Source-hydrophone distance is large enough such that effects of pressure due to water displacement or afterflow are minimized. Also, the source-hydrophone distance is held small relative to both air/water and water/bottom distances which guarantees sufficient boundary reflection attenuation to minimize their effects on the near-field signature.

Four parameters are useful in the evaluation of energy source signatures. These four parameters are (Farriol, 1970):

- a) peak pressure in the primary pulse, P_{max}
- b) the width of the primary pulse at 37 per cent of peak pressure, θ
- c) the bubble period, T
- d) the ratio of peak pressure of the primary pulse, P_{max} to peak pressure of the secondary or bubble pulse, P'_{max}

Figure 1 shows the idealized near-field signature of an explosive source. The secondary and tertiary events or first and second bubble pulses are apparent on the explosive signature. Figure 2 shows the idealized near-field signature of the acoustic signal generated by an isotropic implosion. The amplitude spectra of both signatures is shown below the time domain signature in both figures. P_{max} and θ determine the general level of the amplitude spectrum of the signatures. A high pass cut-off is defined by the bubble period T of the explosive signature. There is no corresponding high pass on the implosive signature. A low pass cut-off is defined by θ on both amplitude spectra. The amplitude of the ripple on the explosive signature varies as a function of the ratio of P'_{max} to P_{max} while its period varies as a function of T .

Figure 3a shows an idealized far-field signature corresponding to the near-field explosive signature of Figure 1. The ghost is reversed in polarity by the negative reflection co-efficient at the air/water interface and lags the direct arrival of the positive pressure pulse by the two-way travel time from the source to the surface. An additional high pass cut-off is introduced by the ghost and is a

BEST AVAILABLE COPY

P_{max} peak pressure in the primary pulse
 θ width of the primary pulse at $.37 P_{max}$
 T bubble period
 P'_{max} peak pressure in the bubble pulse

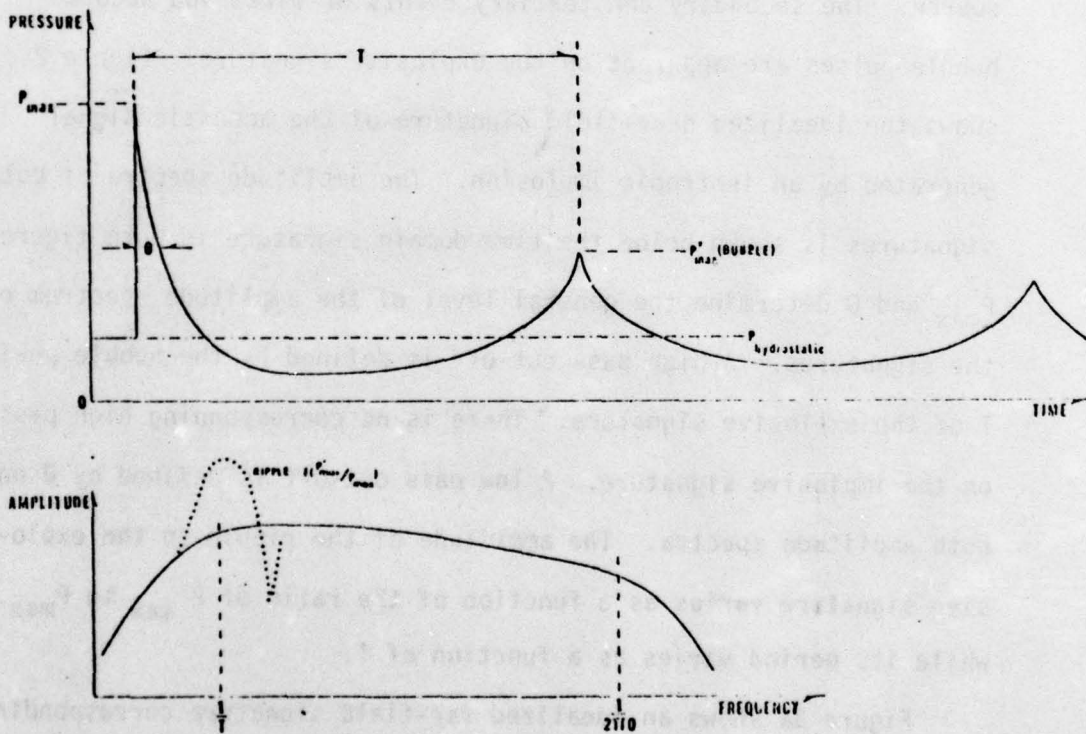


Figure 1. The idealized near-field signature of a typical explosive energy source in the time and frequency domain.

P_{max} peak pressure in the primary pulse
 θ width of the primary pulse at $.37 P_{max}$

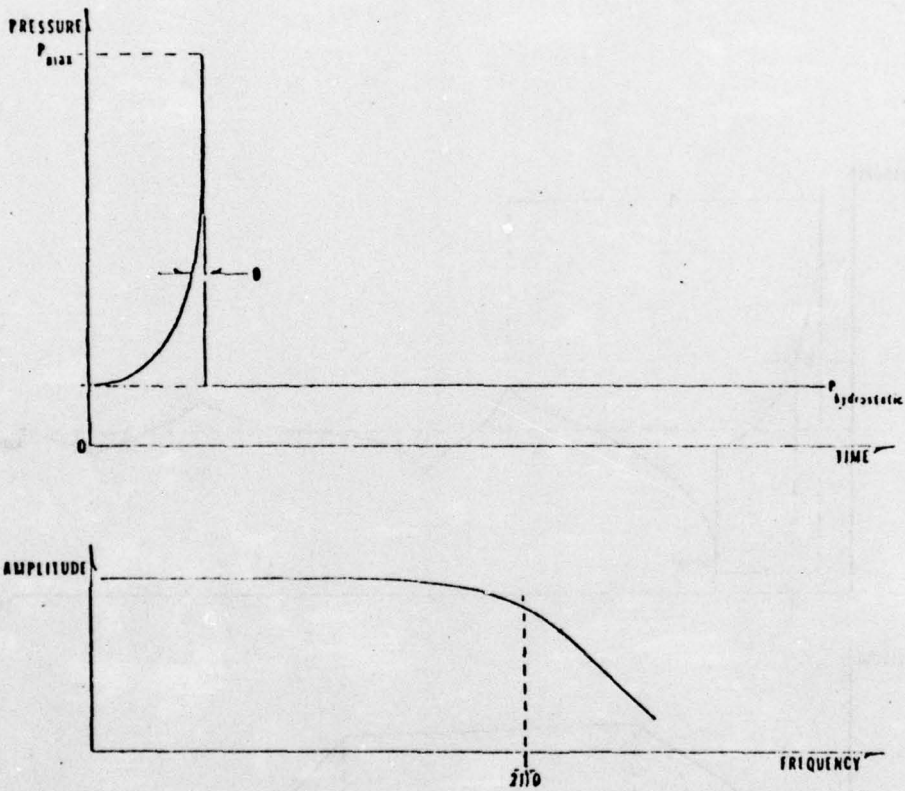


Figure 2. The idealized near-field signature of an isotropic implosion in the time and frequency domain.

- P_{\max} peak pressure in the primary pulse
 θ width of the primary pulse at $.37 P_{\max}$
 T bubble period
 t two-way travel time from source to surface

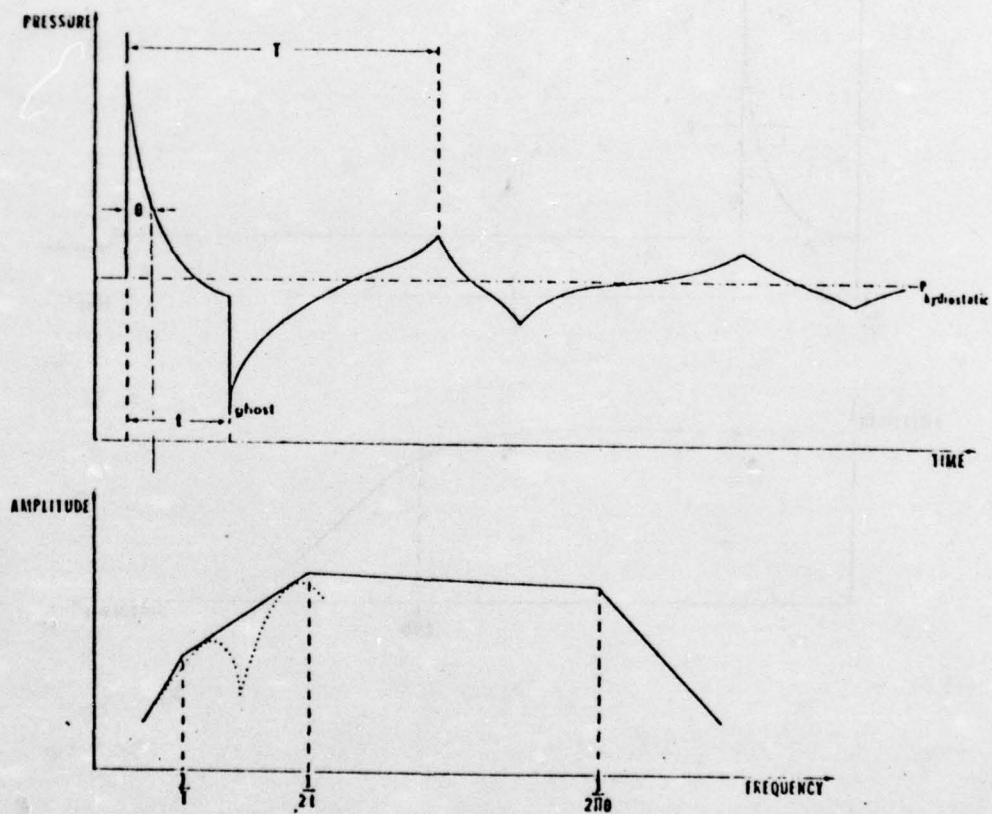


Figure 3. The idealized far-field signature of a typical explosive energy source in the time and frequency domain.

BEST AVAILABLE COPY

- θ width of the primary pulse at .37 peak pressure
- t two-way travel time from the source to the surface

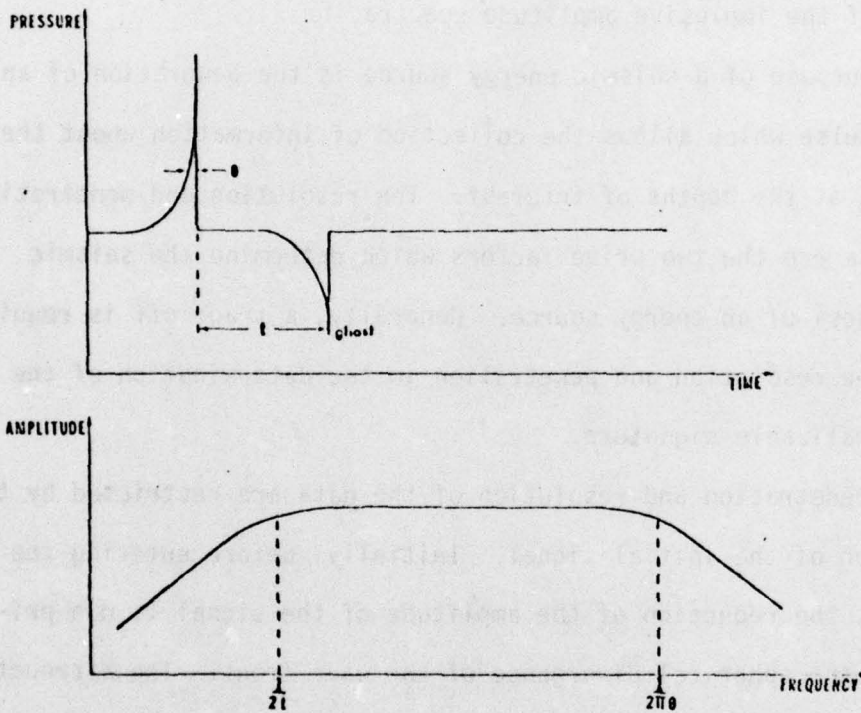


Figure 4. The idealized far-field signature of an isotropic implosion in the time and frequency domain.

function of the time lag of the ghost behind the direct arrival. The effect of the ghost on the envelop of the amplitude spectra of an explosive far-field signature is shown on Figure 3b. Figure 4 shows the effects of the ghost on the amplitude spectra of the far-field signature corresponding to the near-field implosive signature of Figure 2. The ghost-induced high pass determines the low frequency fall-off of the implosive amplitude spectra.

The purpose of a seismic energy source is the generation of an acoustic pulse which allows the collection of information about the subsurface at the depths of interest. The resolution and penetration of the data are the two prime factors which determine the seismic effectiveness of an energy source. Generally, a trade off is required between the resolution and penetration in the determination of the optimum realizable signature.

The penetration and resolution of the data are restricted by the attenuation of the initial signal. Initially, before entering the sea floor, the reduction of the amplitude of the signal is due primarily to the spherical divergence of the wave front. The attenuation due to divergence result in a reduction in amplitude proportional to the inverse of the distance traveled and is frequency independent. After the wave front penetrates the sea floor, material attenuation of Q of the subsurface also contributed to the reduction of signal amplitude. The magnitude of the material attenuation losses increase significantly as a function of frequency, approximately proportional to frequency (Attewell, 1966), and rapidly destroys the high frequency energy of the seismic pulse. Typically, signals with two-way travel times of greater than a few seconds contain no data with energy above 50 or 60 Hz.

Data recovered by a survey is restricted to a frequency band determined by the low cut-off of the far-field signature and the high cut-off imposed by the material attenuation of the subsurface through which the signal passed. The frequency band to which the reflected energy is limited is called the seismic frequency band. Restriction of the data to the seismic frequency band must be considered in the evaluation of the signature of an energy source.

The ability to identify an individual reflector and the amount of information about the reflecting interface is related to the inverse of the time duration of the reflected signal. Referring back to Figures 1 and 2, the inverse relation between the time duration of the signal and the high cut-off of its spectrum is shown. Modification of the original far-field frequency spectrum by the material attenuation of the subsurface significantly lowers the high cut-off of reflected signal. The effect of reducing the upper limit of the band pass of an implosive and explosive far-field signatures is shown in Figures 5 and 6 respectively. A substantial reduction in the resolving ability of the filtered signature is especially apparent in the explosive signature. The almost total attenuation of the initial explosive pulse coupled with the amount of low frequency energy initially present in the secondary events introduces considerably ambiguity into the reflection record. Reduction of the relative amplitude of the secondary events on the explosive record would considerably improve data quality.

The signature of an energy source should be an acoustic pulse which allows maximum practical resolution at the depth of interest. A signature with its energy concentrated in a single impulsive event

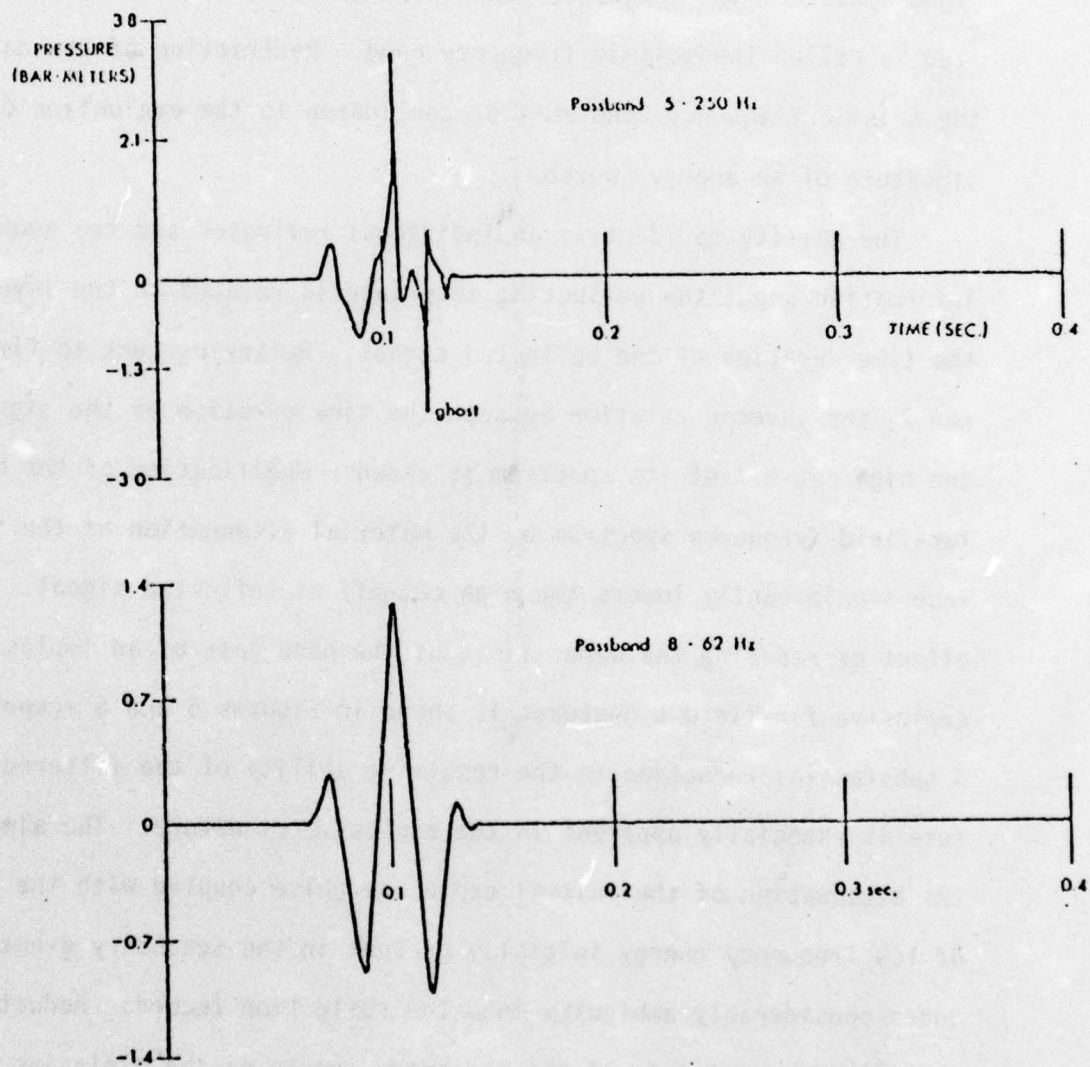


Figure 5. Effects of reducing the passband of an implosive far-field signature (Casius Water Gun from Sodera).

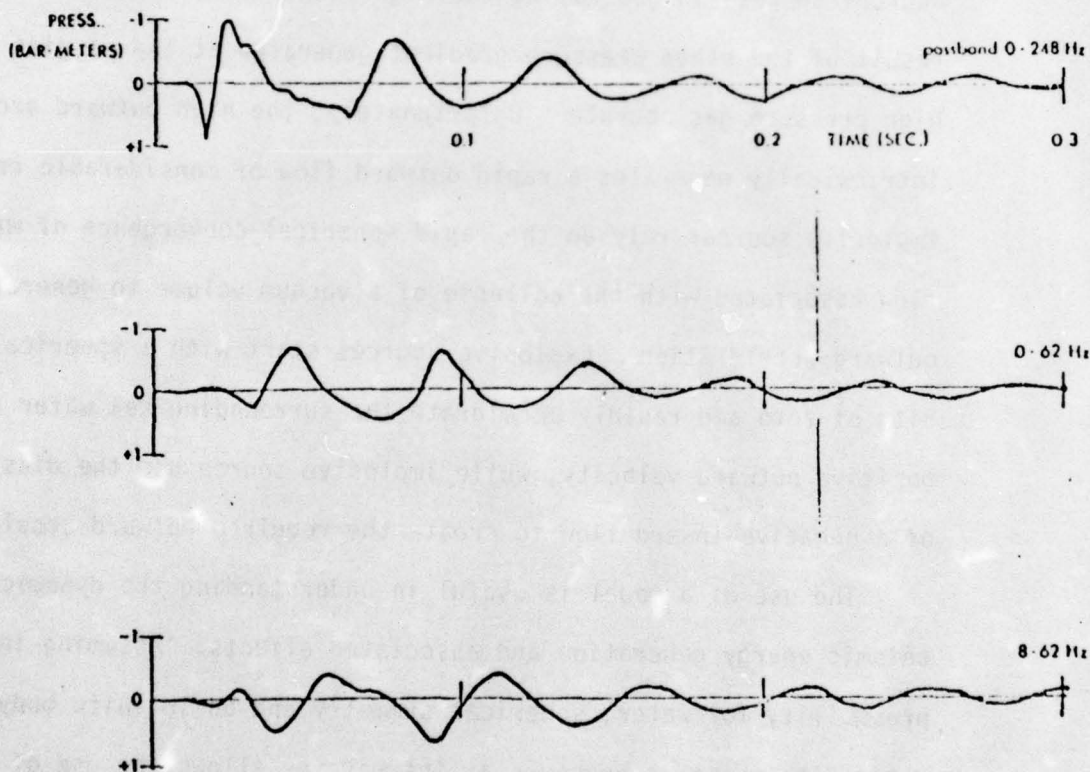


Figure 6. The effects of reducing the passband on the far-field signature of an explosive energy source (40 cu. in. PAR air gun from Giles, 1973).

and a relatively flat spectrum across the seismic frequency band is desired. Ideally, the peak in the power spectrum should be in the higher seismic frequencies to allow greater resolution. The signature should also have a high degree of repeatability to reduce the expense of computer enhancement of the data.

The effective generation of a marine seismic pulse requires that a high outward acceleration be imparted to the sea water. Explosive sources succeed in generating the high outward acceleration as the result of the steep pressure gradient generated at the margins of a high pressure gas bubble. Unfortunately, the high outward acceleration intrinsically generates a rapid outward flow of considerable energy. Implosive sources rely on the rapid spherical convergence of water flow associated with the collapse of a vacuum volume to generate the outward acceleration. Explosive sources start with a spherical velocity of zero and rapidly accelerate the surrounding sea water to a positive outward velocity, while implosive source use the dissipation of a negative inward flow to create the required outward acceleration.

The use of a model is useful in understanding the dynamic of seismic energy generation and associated effects. Assuming incompressibility for water, spherical symmetry and an infinite body of water with constant pressure at its margins allows the use of a less complex model without sacrificing the qualitative value of the results. Three equations will be useful as models with the restrictions just described.

Bernoulli's equation for hydraulic flow (Kramer, 1968):

$$p - P_0 = \frac{1}{r} \frac{\rho}{4\pi} \frac{d^2V}{dt^2} - \frac{1}{r^4} \frac{\rho}{32\pi^2} \left(\frac{dV}{dt} \right)^2 \quad (1)$$

where: p total water pressure at radius r
 from center of bubble
 P hydrostatic pressure
 ρ density of water
 V volume of spherical bubble

can be interpreted as being the sum of two components, one falling off as the inverse of radius and another falling as $1/r^4$. The two components can be interpreted as corresponding to:

- (1) The radiated seismic signal falling off as $1/r$ and being proportional to the volume acceleration.
- (2) Hydraulic afterflow, falling off as $1/r^4$ and being proportional to the volume velocity squared.

The radiated seismic signal is of prime interest but consideration of the effects of the hydraulic afterflow are significant as an energy conservation mechanism. Afterflow is the inescapable result of the spherical divergence inherent in the point source nature of bubble generation. The afterflow serves as a mechanism for the temporary storage of kinetic energy not immediately radiated in the acoustic signal. Another useful form of Bernoulli's equation is

$$p - P_0 = \frac{R}{r} \left(\rho \left(R \frac{d^2R}{dt^2} + 2 \left(\frac{dR}{dt} \right)^2 \right) - \frac{1}{r^4} \frac{\rho R^4}{2} \left(\frac{dR}{dt} \right)^2 \right)$$

where: R radius of the bubble
 p total water pressure at radius r
 from center of bubble
 P_0 hydrostatic pressure

The pressure associated with the radiated acoustic signal falls off as $1/r$. A seismic energy source must impart a high outward acceleration to the surrounding water to be effective. The pressure associated with water displacement, or afterflow, is represented by the second term and falls off as $1/r^4$.

Most present explosive seismic energy sources generate the rapid outward acceleration by either generating or venting high pressure gas in the sea water. The high initial pressure gradient established across the bubble-water interface rapidly accelerates the layer of water adjacent to the bubble outward. As the initial compressional wave travels outward, it compresses the water and upon expansion there is a resulting net outward displacement. Considerable energy is contained in the afterflow generated to compensate for the outward displacement. As the bubble enlarges, internal gas pressure falls off but acceleration of the adjacent water outward continues until internal pressure is equal to the ambient hydrostatic pressure. The kinetic energy stored in the hydraulic afterflow must be dissipated before the initial outward bubble expansion can stop. Afterflow kinetic energy is primarily dissipated by continued bubble expansion, reducing internal bubble pressure below hydrostatic pressure.

Initial bubble expansion terminates as soon as the kinetic energy associated with the hydraulic afterflow has been dissipated. The large amount of energy remaining in the system that hasn't been dissipated by acoustic radiation or thermo-viscous losses is concentrated in the potential energy of the partial vacuum of the bubble. Acting as a result of the negative pressure gradient across the margins of the bubble, an accelerating collapse of the bubble begins. The inward or negative acceleration of the bubble margin continues until internal bubble pressure exceeds hydrostatic pressure. The kinetic energy concentrated in the inward flow of the surrounding water is dissipated by recompression of the gas forming the bubble. The recompression of the gas results in a re-expansion of the bubble and the cycle begins again. Unfortunately,

a significant amount of the energy left in the system expresses itself as a secondary acoustic signal or bubble pulse. The bubble pulse is generated as internal bubble pressure climbs rapidly as a result of the re-compression of the gas.

The gas vented to generate the bubble serves as a pneumatic spring. The peak pressures of each bubble pulse tend to fall off exponentially as a function of the damping of the system. The oscillation of the bubble continues until the energy in the system has been dissipated by the damping effects of acoustic radiation and thermo-viscous losses or the gas is vented at the surface. Figure 7 illustrates the bubble cycle of the typical compressed gas source and its effects on the near-field signature. Equation (2) gives the velocity of the bubble margin as a function of initial gas pressure relative to hydrostatic pressure (Rayleigh, 1917).

$$\left(\frac{dR}{dt}\right)^2 = \frac{2Q}{R^3} \frac{R_0^3}{R} \log \frac{R_0}{R} - \frac{2P_0}{3} \left(\frac{R_0^3}{R^3} - 1\right) \quad (2)$$

$$\left(\frac{dR}{dt}\right)^2 = 0 \quad \text{where:} \quad -P_0 \left(1 - \frac{R_0^3}{R^3}\right) = Q \log \frac{R_0}{R} \quad (3)$$

where: R_0 initial bubble radius
 R bubble radius
 Q initial bubble pressure

The two zeros of (2) are given by (3). If energy was not removed from the system through damping effects, the bubble would oscillate between the two values of R_0/R given by the zeros of (3).

BEST AVAILABLE COPY

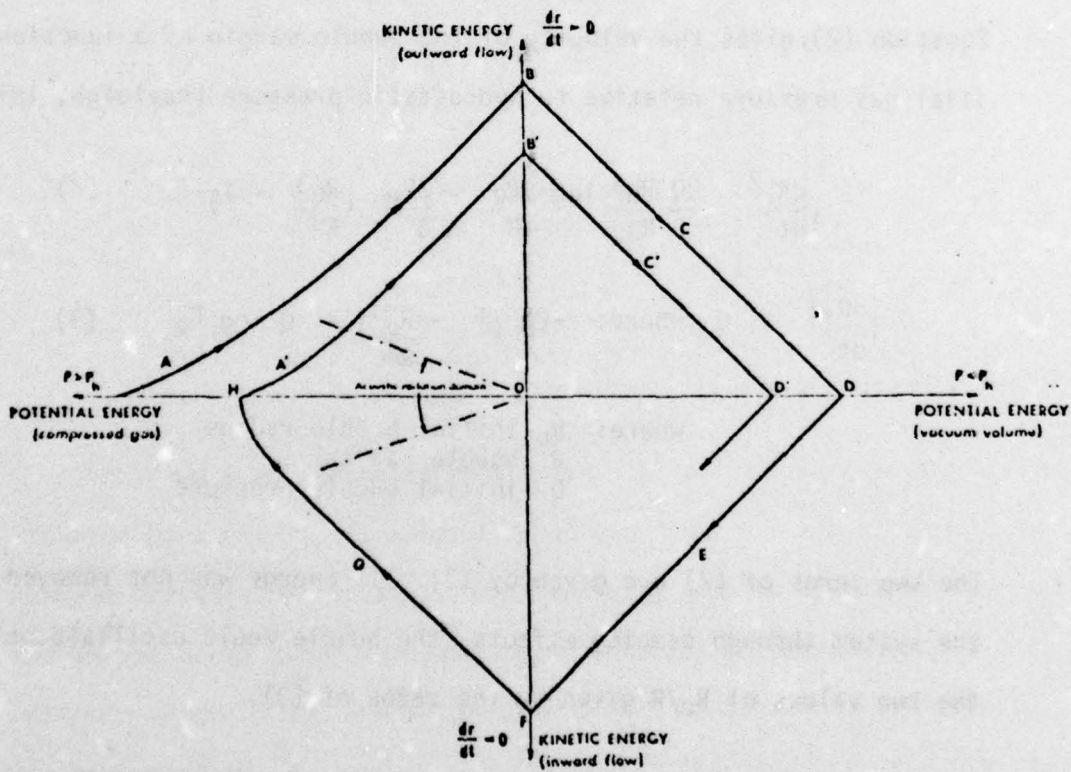
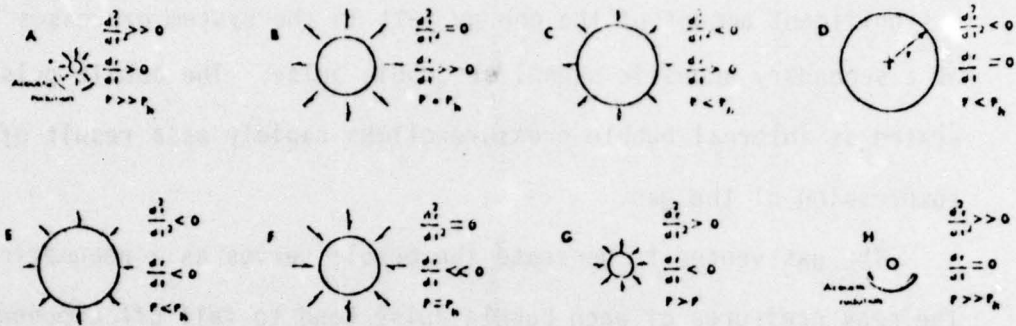


Figure 7. The bubble cycle of a compressed gas explosive seismic energy source.

The major deficiencies of compressed gas sources arise as the result of the secondary events on the signature. Although the high frequency energy is concentrated in the initial event on the signature, the low frequency energy is not. The effects of the material attenuation on the high frequency energy of the explosive seismic pulse rapidly attenuates the primary event. Reduction in the relative amplitude of the bubble pulse has generally been required to improve the resolution of the data. Various methods have been used to achieve the required bubble pulse attenuation. Direct reduction of bubble pulse amplitude is accomplished by compensating for or dissipating afterflow energy, but at the expense of sacrificing considerable energy.

Implosive seismic energy sources use the collapse of a vacuum bubble as the prime mode of seismic energy generation. The cavitation of a vacuum volume is similar dynamically to the bubble collapse but lacks the presence of a compressible gas to regenerate the bubble. The generation of the vacuum bubble must be achieved without significant acoustic generation. The acceleration of the water must be held to a minimum in vacuum bubble generation to limit acoustic effects. Restriction of water acceleration below an acceptable level requires that initial vacuum volume generating mechanism be a relatively long term event to impart sufficient energy to the resulting afterflow. The ability of the hydraulic afterflow to absorb considerable kinetic energy allows it to serve as a convenient energy sink.

Assuming a spherical vacuum cavity is generated, two equations are useful in understanding the subsequent collapse (Rayleigh, 1917).

$$\frac{p}{P_0} = 1 + \frac{(z + 4)^{4/3}}{4^{4/3}(z-1)^{1/3}} \quad (4)$$

$$r = R \left(\frac{4(z-1)}{(z-4)} \right)^{1/3} \text{ for } z > 4.00 \quad (5)$$

$$\frac{p}{P_0} = \frac{z}{4^{4/3}} \text{ for } z \gg 4.00 \quad (6)$$

$$r = 4^{1/3} R \text{ for } z \gg 4.00 \quad (7)$$

where: R_0 = initial cavity radius
 R = cavity radius
 $z = \frac{(R_0)^3}{(R)^3}$
 P_0 = hydrostatic pressure
 p = maximum pressure
 r = radius where maximum pressure occurs

Equation 4 is the relation between maximum pressure in the system, assuming pressure at the water-bubble interface remains at zero. The maximum pressure, P , is at infinity as long as z is less than four. After the value of z has exceeded four, maximum pressure occurs at a finite distance given by (5) and is greater than P . As the cavity fills up, the maximum pressure, p , becomes very large and its magnitude and the radius at which it occurs can be approximated by (6) and (7). The maximum pressure actually achieved in the collapse of a cavity is limited by the effects of the compressibility of water.

The collapse of the vacuum volume is the result of the negative pressure gradient initially established at the margins of the cavity. During the initial stages of the collapse, the gradient has gentle slope and extends outward from the margins of the bubble a considerable distance. As a result of the gradient, inward flow of water is gently accelerated. When the radius of the collapsing cavity is reduced to approximately 1/4 of its initial volume, a region of progressively higher pressure is generated within the water a finite distance from the margin of the collapsing cavity. The high pressure developed in this region is a result of the spherical convergence of the water flow. As the radius of the collapsing cavity decreases, the magnitude of the effects of the spherical convergence near its margins increases. The momentum of the inward flowing water at larger radius acts on the water at smaller radius which is undergoing the effects of the severe spherical convergence. The smaller the radius of the collapsing vacuum volume, the greater the effects of the spherical convergence and the greater the pressure generated as a result. A rapid exponential rise in the generated acoustic signal results from the rising pressure. Upon total collapse, the opposing margins of the bubble collide generating a very short duration, high amplitude "spike" on the signature.

The near-field acoustic signal generated by the collapse of vacuum cavity typically has a very rapid, exponential rise terminating in a narrow, high amplitude spike. Figures 2 and 4 illustrate the idealized signatures. The high frequency, low amplitude acoustic events following the collapse the the primary event on actual signatures (Figure 5) are probably the results of elastic oscillation of the water at the site of

EFFICIENCY

The efficiency of the seismic energy generating system becomes increasingly important as seismic output is increased or as survey vessel size is reduced. Limits on survey capability can become largely a function of the weight of the largest seismic energy source system that can safely be stowed aboard a vessel. Restriction of seismic power output introduced by weight limitations often force a severe compromise between survey speed, penetration, and shot spacing.

The amount of useful seismic power generated per pound system weight primarily reflects the efficiency of converting the output of a prime mover, such as, gas or diesel engine, to desired acoustic power. Overall efficiency generally can be expressed as the product of three factors:

- 1) Power conversion and transport. The ratio of prime mover output to usable power associated with intrinsic energy of restored source and firing rate.
- 2) Conversion of intrinsic source power to acoustic power.
- 3) A factor indicating relative effectiveness of acoustic output i.e. a subjective evaluation of wave form, frequency content, etc.

Most widely used seismic energy generating systems suffer a severe loss of efficiency due to the initial factor, power conversion and transport. Many are caught in a trade-off between (2) and (3), but all leave considerable room for improvement in overall efficiency.

The evaluation of the effectiveness of a seismic energy generating system should also include the vessel modification and support

EFFICIENCY

The efficiency of the seismic energy generating system becomes increasingly important as seismic output is increased or as survey vessel size is reduced. Limits on survey capability can become largely a function of the weight of the largest seismic energy source system that can safely be stowed aboard a vessel. Restriction of seismic power output introduced by weight limitations often force a severe compromise between survey speed, penetration, and shot spacing.

The amount of useful seismic power generated per pound system weight primarily reflects the efficiency of converting the output of a prime mover, such as, gas or diesel engine, to desired acoustic power. Overall efficiency generally can be expressed as the product of three factors:

- 1) Power conversion and transport. The ratio of prime mover output to usable power associated with intrinsic energy of restored source and firing rate.
- 2) Conversion of intrinsic source power to acoustic power.
- 3) A factor indicating relative effectiveness of acoustic output i.e. a subjective evaluation of wave form, frequency content, etc.

Most widely used seismic energy generating systems suffer a severe loss of efficiency due to the initial factor, power conversion and transport. Many are caught in a trade-off between (2) and (3), but all leave considerable room for improvement in overall efficiency.

The evaluation of the effectiveness of a seismic energy generating system should also include the vessel modification and support

logistics required for use. Towing and handling of the overboard portions of the system should be possible using standard shipboard equipment. Ideally, the on-board equipment should require no shipboard power or special modification of the survey vessel except tie-downs.

CURRENT ENERGY SOURCES

The discussion of three seismic energy generating systems will briefly summarize the advantages of the different techniques. Air guns are the most widely used marine seismic energy source. Hydro-Sein*, Vapochoc*, and the Sodera water guns are systems which use the implosive collapse of vacuum volumes but use different mechanisms to generate the initial cavity.

Air Guns

Air guns use the rapid release of a volume of high pressure air into the sea water to generate the seismic pulse. The pressure of the air charge varies from 500 psig--Mobil Magnetic*, 2,000 psig--PAR*, to 8,000 psi for the Seismojet* and Unipulse* guns. Similar to most explosive energy sources, bubble pulse amplitude has proven to limit air gun effectiveness. Reduction of bubble pulse amplitude has been achieved through modifying of afterflow or statistical methods.

Two methods of dissipating afterflow energy to reduce bubble pulse amplitude have been developed. The most widespread afterflow modification technique uses a tuned oriface to throttle the venting of the air chamber (Giles, 1973). The controlled discharge of air into the expanding bubble reduces the magnitude of the vacuum drawn as afterflow energy is dissipated by bubble over expansion. Reduction in vacuum volume potential energy results in a less violent bubble collapse and reduced

*Registered Trademarks Listed in Appendix

bubble pulse amplitude. Reduction in bubble pulse amplitude has also been achieved by surrounding the air gun ports with a perforated enclosure or cage. Afterflow energy is dissipated by viscous damping as water flows through holes in the enclosure. Although both throttling devices and cages significantly reduce the relative amplitudes of bubble pulses, a considerable reduction in the initial pulse amplitude limits the use of these techniques.

Firing an air gun at a very shallow depth is a technique capable of eliminating secondary acoustic events. Shallow firing of the air gun allows the resulting bubble to vent to the atmosphere before the bubble's initial collapse. Venting of the bubble at the surface eliminates any subsequent oscillation and acoustic emission. Two factors severely limit the use of shallow firing. The reduction in effective coupling, resulting from surface unloading effects, significantly reduces the amplitude and energy of initial seismic pulse. At shallow depths, the two-way travel time to the air/water interface is short. The time delay of the ghost is not sufficient to isolate it from the primary seismic pulse and results in a destructive interference between the two acoustic events. Generally, the loss in energy due to the unloading and primary ghost interference inherent in shallow firing have resulted in the use of other bubble pulse suppression techniques.

Statistical techniques which result in the relative attenuation of bubble events are in widespread use. The period of bubble oscillation is a function of intrinsic air gun energy and depth at which it is fired. The signatures of a number of different air guns of various chamber volumes are stacked with their primary pulses in phase. Since the bubble

periods vary, secondary events stack out of phase. The net result is the enhancement of the primary signal without significantly increasing bubble pulse amplitude. Reductions in the ratio of bubble pulse energy to primary pulse energy is a function of the number of guns in the array.

The efficiency of air gun systems suffers primarily as the result of the use of high pressure air. The efficiency of commercial 2,000 psi compressor units is generally in the five to ten per cent range. Losses are primarily the result of re-expansion due to mechanical clearances and thermal effects. The efficiency of an 8,000 psi system would be lower than the 2,000 psi units.

The efficiency of intrinsic air volume energy-acoustic energy conversion of air guns is one of the highest for artificial explosive sources (Kramer, 1968). The use of bubble pulse suppression devices to improve the quality of the acoustic signal reduces efficiency significantly. Typical reductions in primary peak pressure are about 4dB for throttling devices or cages (Giles, 1973).

Air guns using 10 inch³ chambers or less use considerably more air than their chamber size would indicate. The acoustic effectiveness of the additional air used is minimal. The resulting waste of compressed air can reduce efficiency of a system using a 1 inch³ chamber by over 200 per cent.

Air guns are one of the most widely used seismic energy generating systems. The effects of bubble oscillations on the signature can be minimized, reliability is high and the acoustic output is highly repeatable. Shipboard equipment is large and bulky but is relatively reliable, simple, and safe. The use of arrays is restricted to larger vessels which have equipment to deploy the array and sufficient

displacement to carry the compressor system. Recent demands for data of greater penetration and resolution have required the use of extremely large compressors. Large commercial operations have reached a point where, even with specialized survey vessels, limits on compressor size have forced compromise in data quality. Surveys conducted from small vessels must contend with severe trade-offs between acoustic power, acoustic quality, and survey speed.

Vaporchoc

The use of steam to generate a vacuum volume for implosive generation of an acoustic signal was investigated by Raytheon for the United States Navy in the early 1960s (ONR, 1965). Vaporchoc*, a commercial seismic energy generating system using similar techniques was developed in France and introduced in the late 1960s (Farreol, 1970). The acoustic signal is generated by the injection of a large quantity of steam into the sea water. Injection of the steam forms an expanding steam bubble. When the steam supply is turned off, the steam holding up the bubble cools and condenses very quickly, resulting in a partial vacuum. The cavity implodes, generating an acoustic pulse. Bubble oscillations do not occur since all the steam has condensed before the cavity has totally collapsed.

Figure 8 shows the far-field signature of the Vaporchoc* system. A low amplitude acoustic event, approximately 50 msec. before the primary event, is generated during the injection of steam. The primary acoustic pulse is typical of the impulse generated by implosive energy sources.

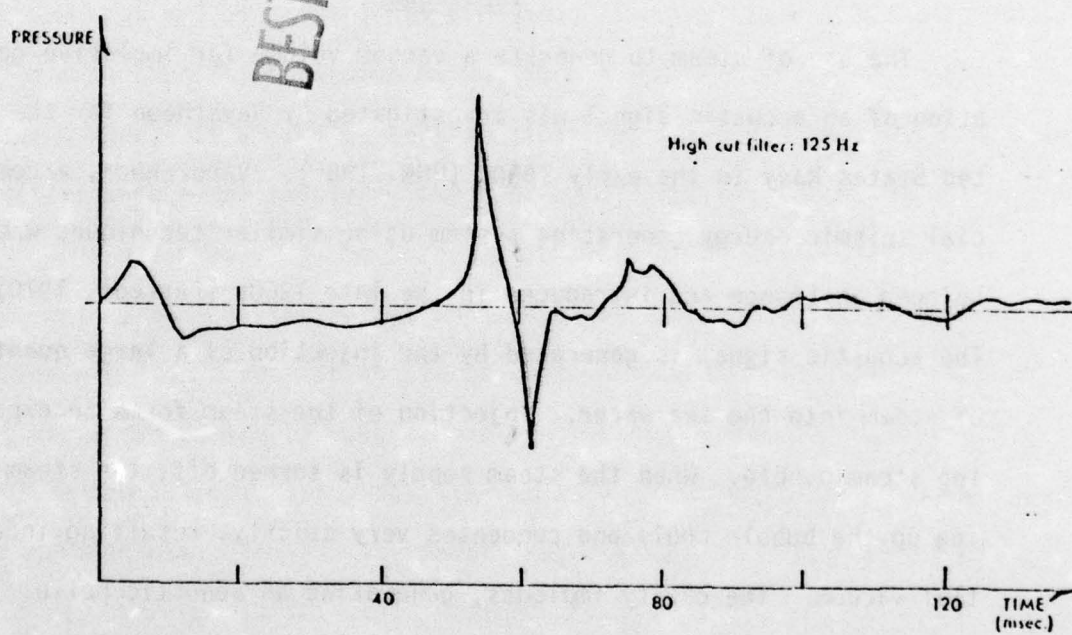


Figure 8. The far-field signature of the Vaporchoc* (Farriol, 1970).

The efficiency of systems using the injection of steam to generate an implosive signal suffers from thermal losses. The thermal losses associated with the transport of steam to the venting valve and during "quiet" bubble generation reduce overall efficiency. A large shipboard boiler is required to supply sufficient steam and restricts the use of the system to larger extensively modified vessels.

Hydro-Sein*

A different approach to vacuum volume generation was used by Marine Geophysical Services in the design of their Hydro-Sein* system. The Hydro-Sein unit uses a hydraulically restored high speed actuator to rapidly separate two plates (Schampf, 1968). A vacuum volume is formed between the two plates which collapses generating a typical implosive acoustic pulse. Presumably, some low-level acoustic event would result from the rapid acceleration of the metal plates. The use of hydraulic power to restore the system enhances the efficiency of the system, but considerable energy is lost in accelerating the relatively heavy, moveable plate assembly. Large elevators are required for deploying the Hydro-Sein units and extensive vessel modification is required.

Sodera - Water Guns

Sodera recently introduced their line of water guns (Sodera, 1973). The Sodera guns use the rapid ejection of a water plug into the sea water to generate a vacuum volume. An air gun is mounted with its venting port behind a floating piston. The compressed air vented from the air gun rapidly drives the piston outward ejecting the water plug.

Motion of the ejected water plub in the sea water draws a vacuum behind it. The acoustic pulse is generated by the subsequent collapse of the vacuum volume.

The far-field signature of Soder's Casios Water Gun* is shown in Figure 5. Similar to other implosive sources, the signature exhibits a narrow high amplitude primary pulse. The power spectrum of the Casios Water Gun* is flat in the seismic frequency band and has its peak power in the 40 to 50 Hz range. Figure 9 shows a comparison of the water guns dB spectrum and an array of 16 air guns. The amplitude spectra are similar with the Casios Simplon having more energy concentrated in the high frequencies. It should be kept in mind that air gun array required 16 guns to reduce the ripple on the spectrum to the degree shown.

The efficiency of the Soder in conversion of compressed air intrinsic energy to acoustic output appears to be approximately the same as a large air gun array. It should be kept in mind that the Soder system required the towing of only a single water gun. Reports indicate that problems with reliability has limited widespread use of the Soder system (Chelminski, 1975). The Soder Water Gun, like air gun systems, requires large quantities of compressed air.

BEST AVAILABLE COPY

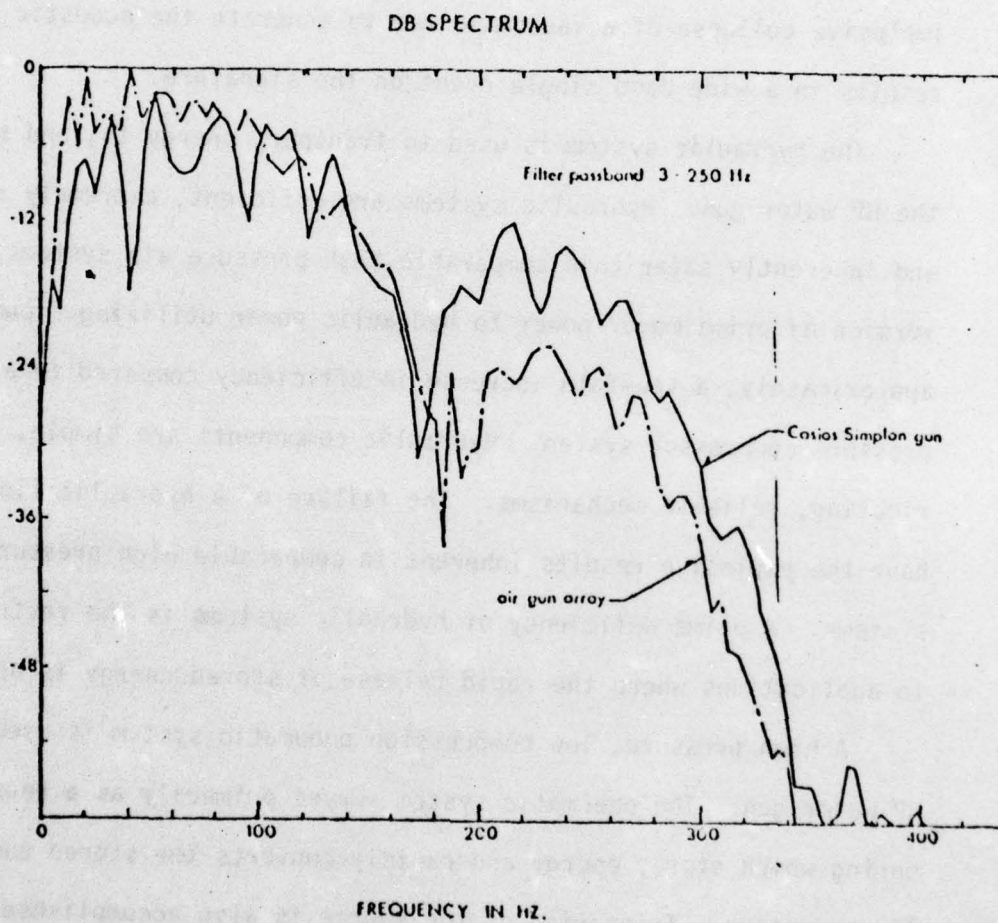


Figure 9. Comparison of the db. spectrum of a 16 unit air gun array (total volume 628 c. in.) and the Casios Simplon Water Gun* (volume 600 cu. in.) fired at 150 atm. (Sodera, 1974).

THE HP SYSTEM

The HP water gun offers two prime advantages over other marine seismic energy sources. A dramatic increase in efficiency is attained by the incorporation of a hydraulic system rather than a high pressure pneumatic system as the prime energy conversion medium. The use of the implosive collapse of a vacuum volume to generate the acoustic pulse results in a wide band single event on the signature.

The hydraulic system is used to transport energy to, and restore, the HP water gun. Hydraulic systems are efficient, extremely reliable, and inherently safer than comparable high pressure air systems. Conversion of prime mover power to hydraulic power utilizing a pump offers, approximately, a ten-fold increase in efficiency compared to a high pressure compressor system. Hydraulic components are simple, self-lubricating, reliable mechanisms. The failure of a hydraulic line doesn't have the explosive results inherent in comparable high pressure air systems. A prime deficiency of hydraulic systems is the restriction to applications where the rapid release of stored energy is not required.

A high pressure, low compression pneumatic system is used in the HP water gun. The pneumatic system serves primarily as a reusable spring which stores energy and rapidly converts the stored energy into linear motion. Triggering of the source is also accomplished through the pneumatic system. The pneumatic system is restricted to a very low compression ratio to eliminate the thermal and mechanical losses normally associated with high pressure air systems. A supply of high pressure air is required to initially charge the chamber of the water gun and to

replensih losses due to restoring the water gun. Losses due to restoring the source is less than .05 cu. in. per shot.

The rapid ejection of a water plug from the water gun generates a vacuum volume which implodes. Efficiency in the conversion to intrinsic energy of the ejecting mechanism to acoustic energy is better than air gun systems. The acoustic energy is also inherently concentrated in a single, high amplitude, narrow pulse. Concentration of the energy in a wide band signal coupled with the increase in efficiency of the overall system indicates a possible evolution of the prototype into a valuable exploration tool.

Description and Operation

The HP water gun uses the rapid injection of a volume of water or water plug into the sea water to generate the vacuum volume. Figure 10 shows a simplified cross section of the water gun. The water plug is ejected from the muzzle by the rapid outward acceleration of the air-water piston assembly. Restoring of the air-water piston assembly is performed by the hydraulic cylinder assembly. The operation cycle is diagrammatically shown in Figure 11. The hydraulic and air support system shown in Figure 12 and the electrical control system is shown in Figure 13.

The operational cycle of the HP water gun can be divided into six components. Figures 10 and 11a show the gun restored and ready to fire. Air pressure in the pressure vessel is at its maximum as the air-water piston displaces, approximately, one-tenth total air volume within the vessel. Design of the prototype limits maximum air pressure to 2,000 psi.

The air-water piston is held against the bottom face of the valve housing by the high pressure air (Figure 10). During restoring and before triggering, the restoring air solenoid valve is open. The volume inside the face seal and between the air-water piston and valve housing is vented to one atmosphere through the restoring air solenoid valve. The diameter of the face seal, D_1 , is about 1/2 inch larger than the outside diameter of the piston body, D_2 (Figure 14). An effective area of approximately 2.5 sq. in. is exposed to the high pressure air holding the piston and valve housing together.

The water gun is triggered by closing the restoring solenoid valve and opening the firing solenoid valve. High pressure air is rapidly injected into the volume inside the face seal. The force holding the air-water piston and valve housing together is destroyed and the two separate (Figure 14). High pressure air now can act on the end of the air-water piston. The air-water piston is rapidly accelerated outward and pushes the water out of the muzzle cylinder (Figure 11b). Interaction between the sea water and the ejected water plug causes the flow to diverge.

The air-water piston is suddenly stopped by the muzzle brake at the end of its stroke. Momentum carries the ejected water plug away from the muzzle. Interaction between the sea water and water plug cause continued divergency of the initial linear flow. The kinetic energy of the ejected plug is dissipated as the vacuum volume is generated. Figure 11c shows the vacuum volume after the divergent flow has been totally dissipated. The subsequent implosion of the vacuum volume generates the acoustic radiation (Figure 11d).

The triggering of the water gun also causes the valve control to switch the two-way master control valve. High pressure output from the hydraulic pump is now applied to the upper chamber of the hydraulic cylinder (Figures 12 and 13). The valve housing hydraulic ram is "pushed" into the high pressure air chamber until the valve housing strikes the end of the air-water piston (Figure 11e). A rise in hydraulic pressure caused by the stopping of the ram is detected by pressure switch A (Figures 12 and 13).

The signal from pressure switch A results in the opening of the restoring solenoid valve. A 30 msec. delay retards switching of the two-way master control valve until pressure inside the face seal has dropped to approximately one atmosphere. The valve housing and air-water piston are again held together. High pressure output from the hydraulic pump is applied to the lower chamber of the hydraulic cylinder. The valve housing-hydraulic ram "pulls" the air-water piston into the high pressure air chambers (Figure 11f). The restoring cycle is completed when the ram is stopped and a rise in hydraulic pressure is detected by pressure switch B (Figures 12 and 13). The function control box (Figure 13) allows either automatic or external triggering of the water gun. Automatic triggering permits the maximum firing rate of three seconds per shot. The water gun can also be manually triggered. A hold-restore override is used to stop triggering of the source and to insure the source is unrestored for deployment or retrieval.

Two small compressors driven off of the primary hydraulic power system supply the air requirements of the water gun (Figure 12). Initial charging of the pressure vessel and storage tank to 1,000 psi

takes approximately four minutes. Air lost by restoring, approximately 0.05 in.³/shot, is replenished from the onboard storage tank. The compressor system was used to fire a 10 cu. in. PAR* air gun. The compressors were capable of firing the air gun at a sustained firing rate of once every 17 seconds.

Figures 15 and 16 are photographs of the system. The physical parameters of the HP system are given below:

A. System

1. total weight 1,050 lbs.
2. deck space 15 ft.²
3. gas engine output (estimate) 10 hp. air cooled

B. Source

1. total weight 300 lbs.
2. length 6 ft.
3. volume hydraulic fluid/cycle approximately 0.5 gal.
4. maximum intrinsic energy 18,000 ft. lb./shot
(10,000 ft. lb./shot with present hydraulic pump unit)

Figure 10. Simplified cross section of the prototype HP water gun.

AD-A040 048

WISCONSIN UNIV MILWAUKEE DEPT OF GEOLOGICAL SCIENCES
MARINE GEOPHYSICAL INSTRUMENTATION.(U)
DEC 76 R J WOLD

F/G 17/10

N00014-67-A-0128-0016

UNCLASSIFIED

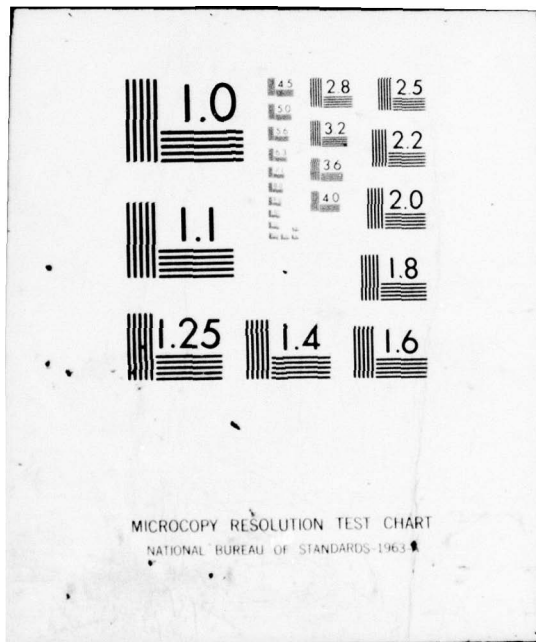
NL

2 OF 2
AD
A040048

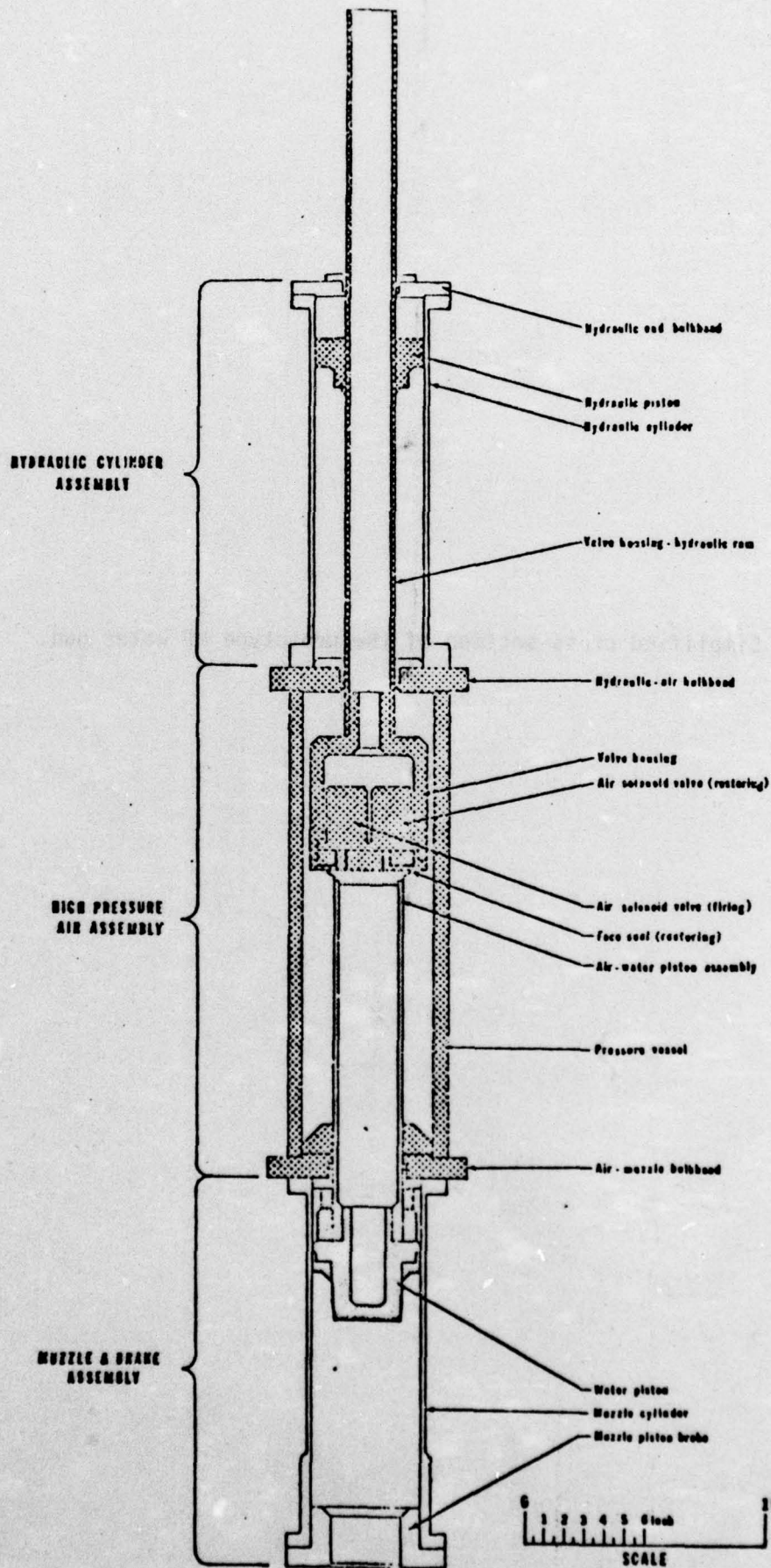


END

DATE
FILMED
6-77



MICROCOPY RESOLUTION TEST CHART
NATIONAL BUREAU OF STANDARDS-1963-A



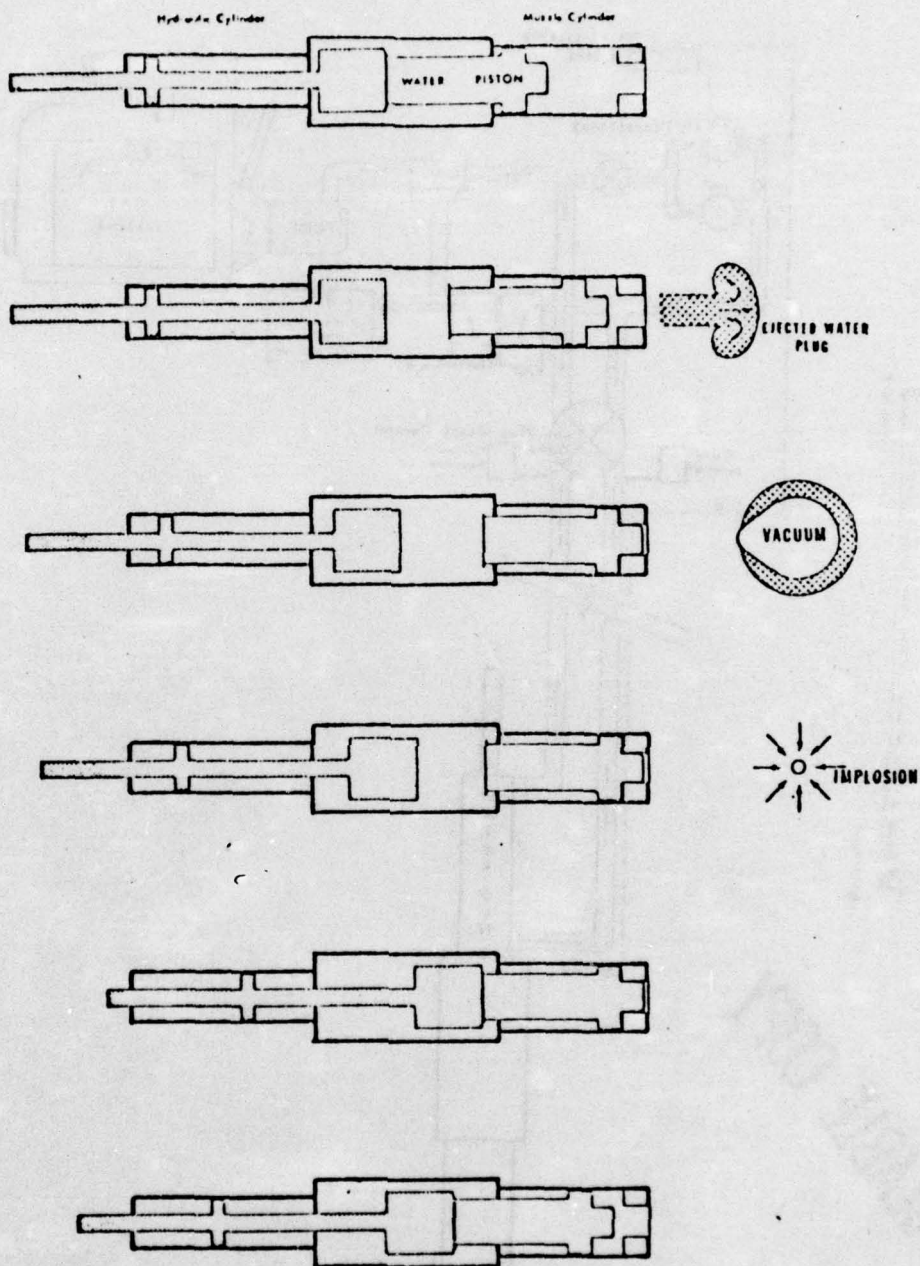


Figure 11. The operational cycle of the HP water gun.

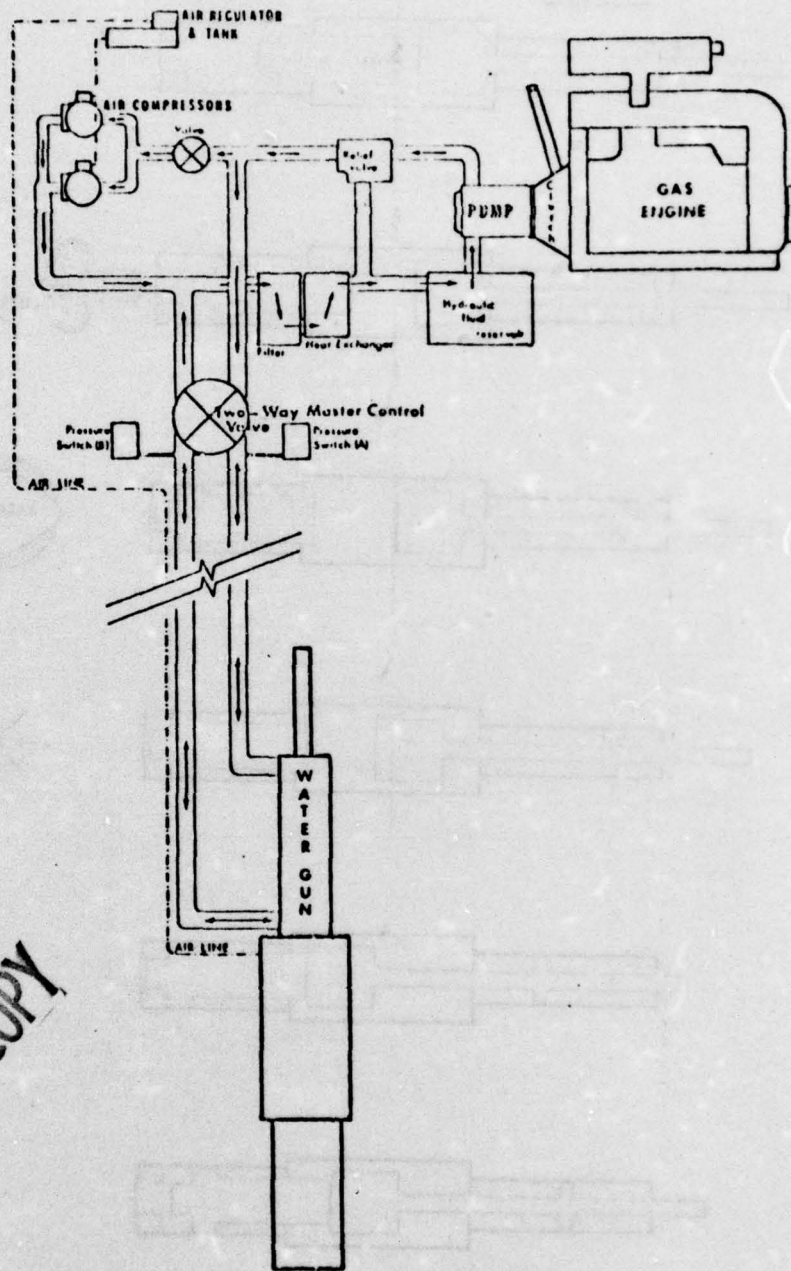


Figure 12. The schematic of the hydraulic and high pressure air systems of the HP water gun.

BEST AVAILABLE COPY

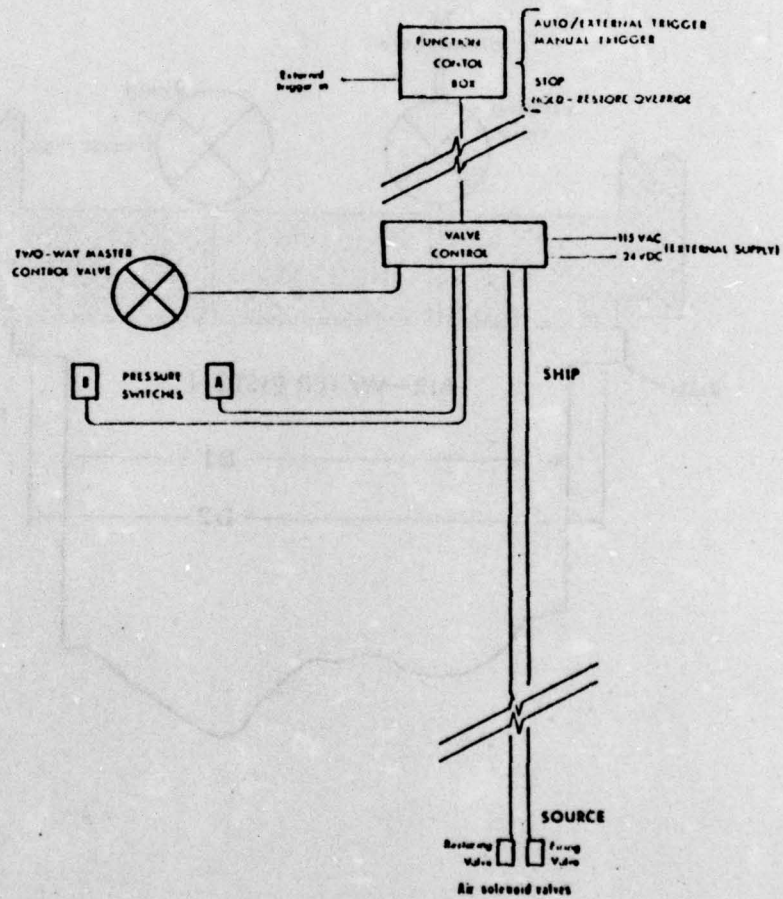


Figure 13. The schematic of the electrical control and monitoring system of the HP water gun. Pressure switches A and B monitor hydraulic line pressure.

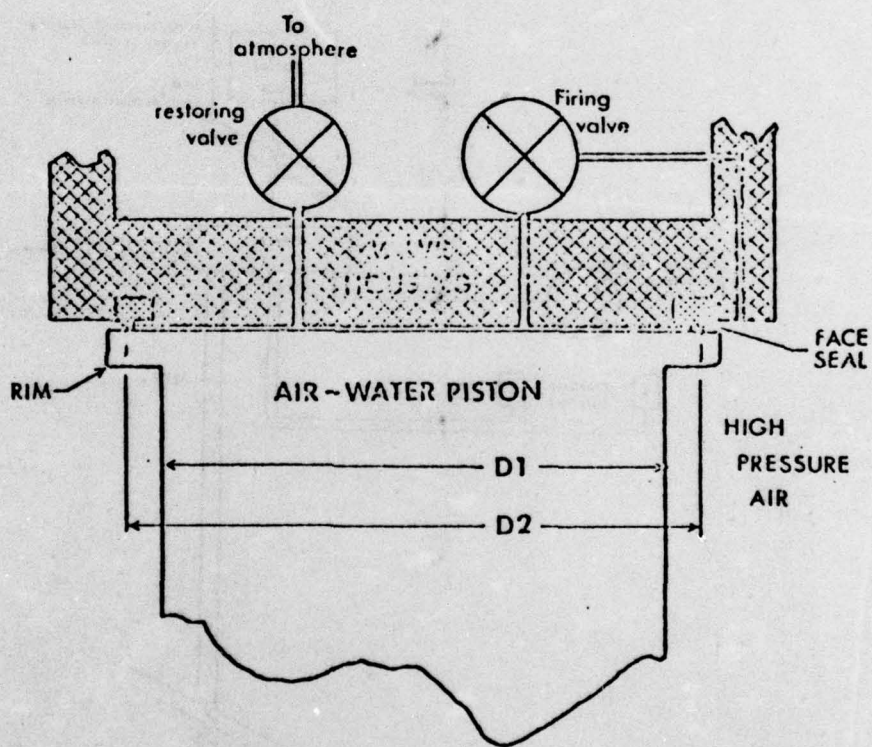


Figure 14. Detail cross section of the face seal between the air-water piston and the valve housing. D1 is the diameter of the air-water piston and D2 is the diameter of the face seal.

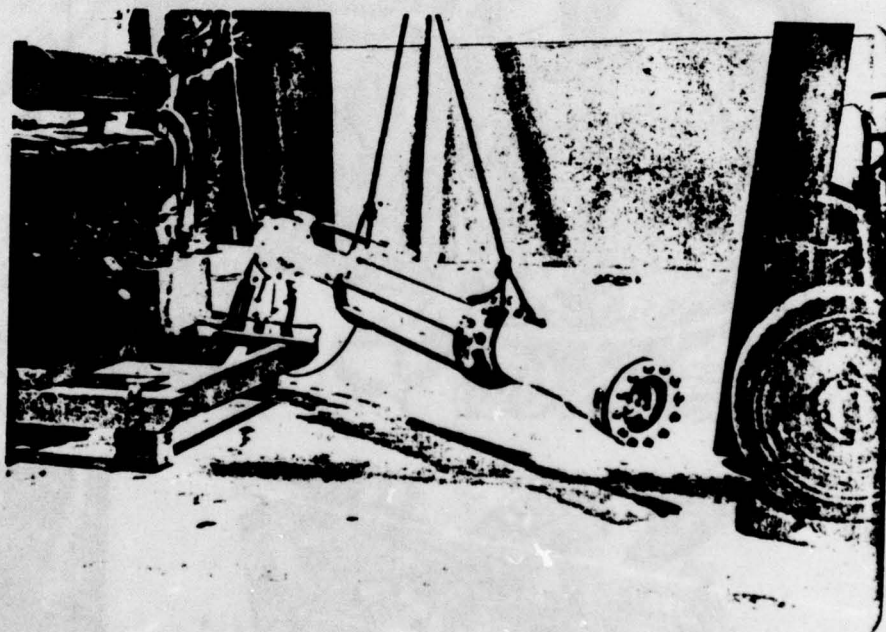


Figure 15. Photograph of the HP water gun.

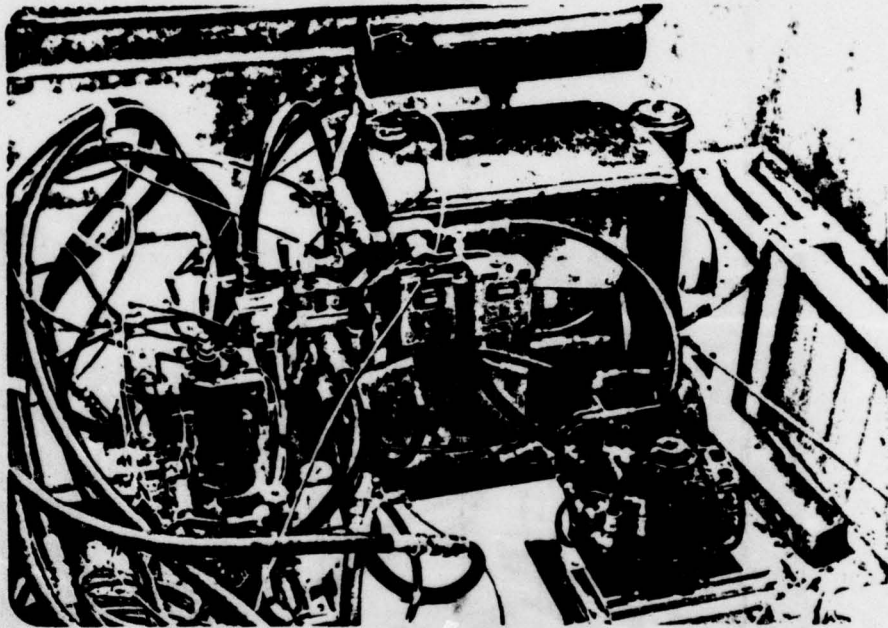


Figure 16. Photographs of the HP system.

FIELD TEST

Field tests of the HP water gun were conducted both in Lake Michigan and on the east coast. The initial test was conducted in Lake Michigan. Although the HP system functioned well, data collected on the Lake Michigan trial was severely distorted by the recording system. The acoustic effect on the survey vessel's hull of the water gun was noticeably louder than the effect of 10 cu. in. air gun fired at 2,000 psi during this test.

Tests were again conducted near Woods Hole, Massachusetts. The second set of tests met with partial success. A Celesco LC* - 32 calibrated hydrophone was used and peak pressures were calculated. A schematic of the electronic equipment used during the second test is shown in Figure 18.

The broad band far-field signature of the HP water gun is shown in Figure 19. A peak pressure of 1.6 bar-meters was calculated for the signature. Tests were limited to maximum air charge pressures of 800 psi by difficulties with the hydraulic supports system.

Visual comparison of the HP signature with the signature of a 40 in.³ air gun (Bolt Associates, 1975) indicates considerably greater energy in the HP signal. An initial even precedes the primary acoustic pulse and is generated by the rapid ejection of the water plug. The initial pulse peak pressure is over 8 db down from the peak pressure of the primary pulse.

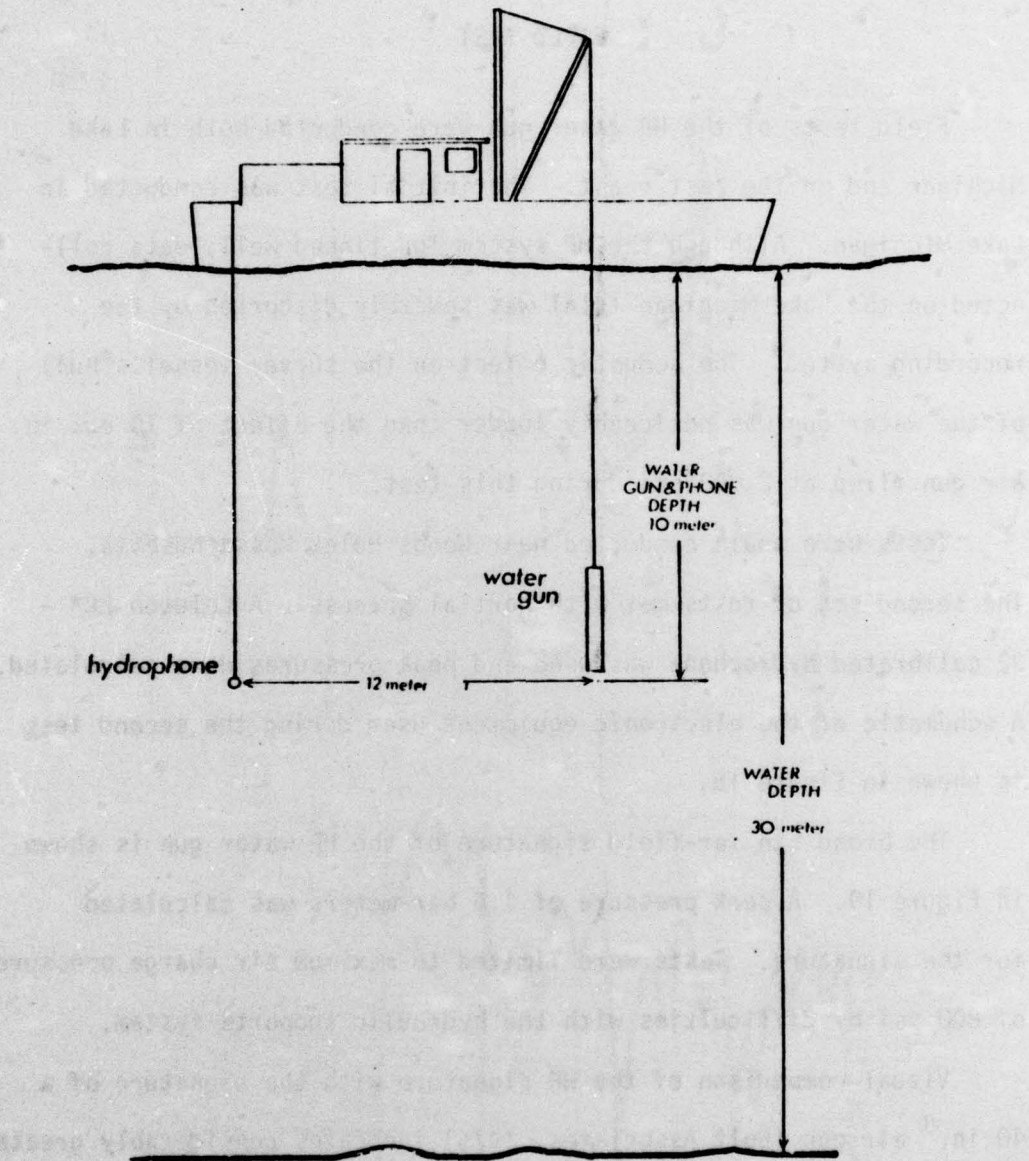


Figure 17. Schematic of the hydrophone/water gun during testing.

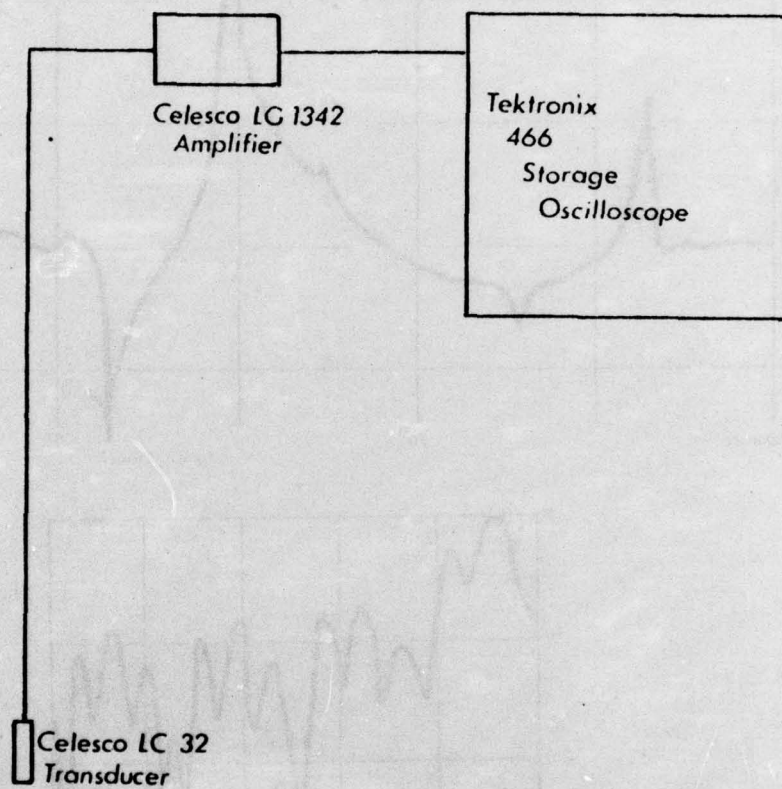


Figure 18. Schematic of the electronic equipment used during tests.

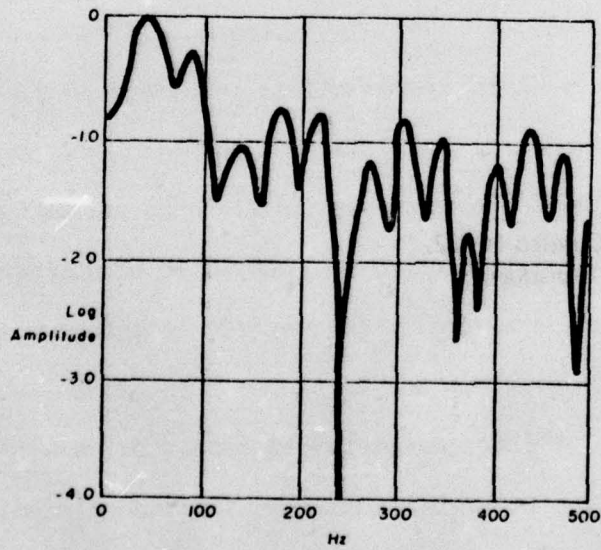
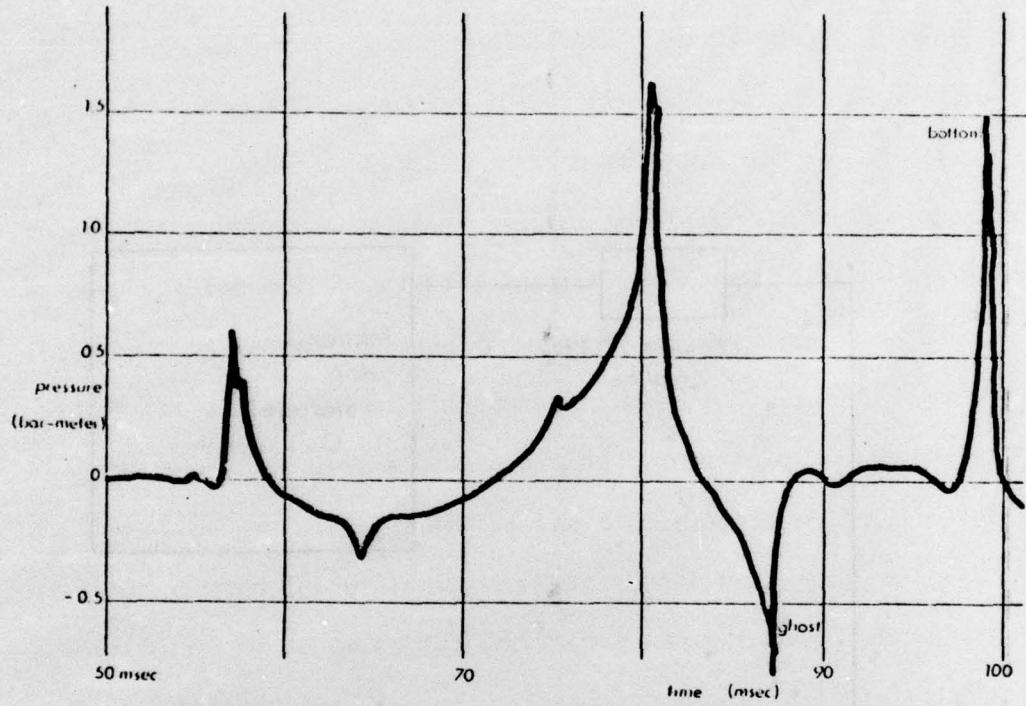


Figure 19. The far-field signature of the HP water gun fired at 800 psi.

The results obtained from the field tests show that the HP system has the potential to warrant further development. A number of deficiencies in the prototype were discovered during the field tests. The design of a higher energy unit has been partially completed and is designed to eliminate the deficiencies found in the prototype.

COMPARISON OF PROTOTYPE AND NEW DESIGN

The design of the prototype was aimed exclusively at the fabrication of a workable test unit in the time span available. A number of compromises were made in the design to allow the use of off-the-shelf materials and also allow most of the fabrication to be performed on campus. The next model will incorporate a number of changes, both the result of lessons learned from prototype evaluation and as a result of the relaxation of time restrictions.

The prototype uses a double acting hydraulic cylinder to restore the air-water piston. Initially, the double acting hydraulic cylinder was incorporated to obtain maximum efficiency but resulted in handling difficulties and an excessive increase in weight and length. The two hydraulic hoses required were difficult to handle and the exposed hydraulic ram was easily damaged.

A single acting hydraulic system requiring only a single hydraulic hose has been designed for the new model. The single acting system uses the valve housing as a piston and reduces the number of seals required. A comparison of 20,000 ft. lb. prototype (Figure 10) and the 150,000 ft. lb. new design (Figure 20) illustrates the reduction in size achieved primarily as a result of the modification. The new design uses the hydraulic system to recompress the air charge. A slight expansion of the air charge then pushes the valve housing and air-water piston to the fully restored position. All sealing surfaces are also protected from damage in the new design.

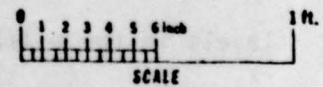
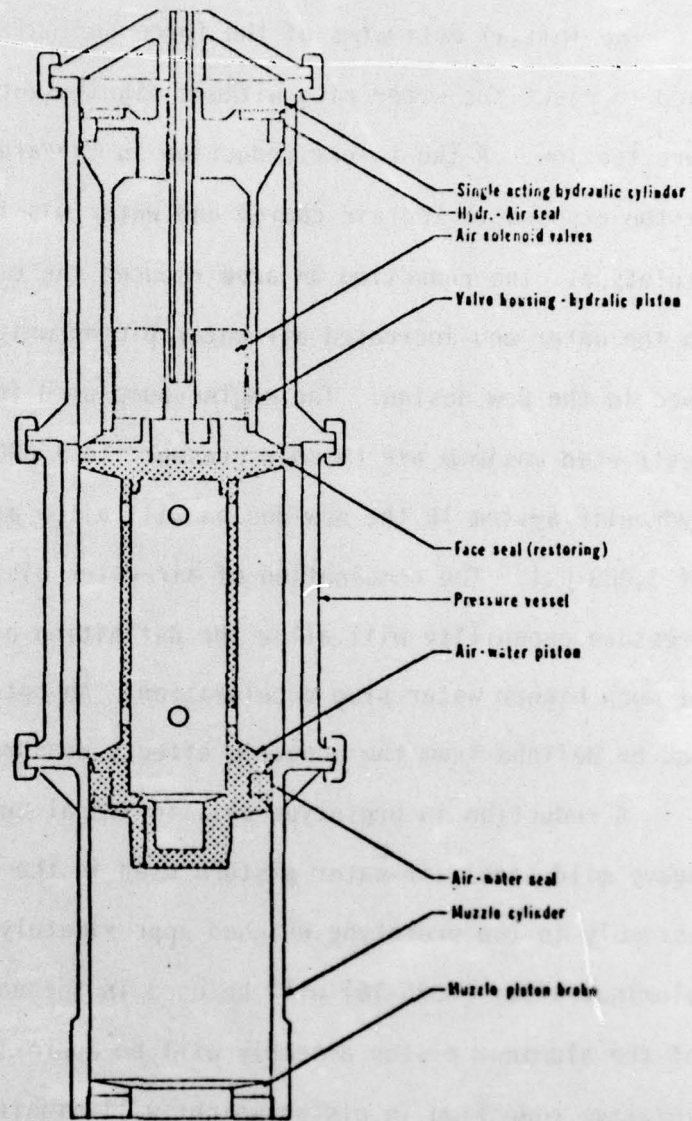


Figure 20. Cross section of the new design. The new design will have an intrinsic energy of 150,000 ft.-lb. when fired at 3,000 psi. internal pressure.

The initial estimates of the force per unit area that could be used to eject the water plug without significant acoustic generation were too low. A two-to-one reduction in the areas of the air-water piston exposed to the air charge and water was incorporated in the prototype. The reduction in area reduced the effective force acting on the water and increased air-water piston weight. No reduction was used in the new design. The engine-pump used in the prototype restricted maximum air chamber pressure to 1,000 psi. A 3,500 psi hydraulic system in the new design will allow air chamber pressures of 3,000 psi. The combination of air-water piston design and high pressure capability will allow the definition of the acoustic effect of much higher water plug acceleration. An optimum operating pressure can be defined from the acoustic effects measured.

A reduction in prototype seismic signal output resulted from the heavy mild steel air-water piston used in the prototype. The piston assembly in the prototype weighed approximately 30 lbs. A high tensile aluminum alloy (7075-T6) will be used in the new design. Total weight of the aluminum piston assembly will be approximately 25 lbs. The relative reduction in piston weight will significantly reduce stress levels in the muzzle brake assembly and increase the efficiency of the new model.

Difficulties were encountered with the dynamic seals in the prototype. The surface finish on dynamic surfaces was not to seal manufacturers' specification. Poor surface finish resulted in minor leaks. The lack of venting between compound (two-way) seals resulted in air leaking into the hydraulic system. Air in the hydraulic system

resulting in foaming and twice required shutting the system down and bleeding the air from the entire hydraulic system. The new design vents the volume between compound seals to either hydrostatic or atmospheric pressure. The venting will prevent minor leaks from effecting the operation of the system.

Corrosion resistance was not considered in the design of the prototype. The use of mild steel, aluminum, and bronze required the prototype to be rinsed off and sprayed with a lubricant after each use. All exposed components of the new model will be fabricated from stainless steel, ideally, a SAE 51431 alloy. All dynamic surfaces will be Delrin (trademark DuPont Co., Inc.) on stainless steel.

Ease of servicing and seal replacement was not considered in the prototype design. All connections were made with bolts where possible. Disassembly of the prototype into major components required approximately one hour and the use of an overhead hoist. The new design uses "U"-shaped collars to secure the major components of the new source. Use of these collars will significantly reduce servicing time. Reduction in size and weight of the new design will allow disassembly and servicing without the use of an overhead hoist.

The elimination of difficulties encountered in the prototype coupled with ideas which evolved during prototype fabrication and testing should allow the eventual use of the new model as a field unit. Seal design in the new model allows latitude for gland redesign without major modification of other components. Integrity of the dynamic seals appears to be the major goal which must be achieved in the new model. A considerable amount of time has been extended

in seal material selection and gland design. At the present time, it appears that, if sealing difficulties are not encountered, the new model will be an effective field unit.

CONCLUSION

The use of a combination hydraulic/pneumatic system to generate seismic energy offers a combination of signal quality coupled with operating efficiency not available in other systems. Although only limited field tests were conducted, analogies drawn from the signal characteristics of Soderia Water Gun indicate the high quality signature the HP system's implosive mechanism can generate. Calculations indicate the prospect of over a 1,000 per cent increase in overall efficiency possible for the HP system over both air gun and Soderia systems.

The prototype system did not undergo any long-term reliability evaluation. A prime motivation for construction of a new model is to have a field system for long-term operation evaluation. If the reliability of the system can attain the reliability of air gun systems, significant improvement in seismic energy generation will have been achieved.

SUGGESTIONS FOR FURTHER STUDY

1. The development of a field system capable of continuous operation over a long period of time.
2. An investigation of the potential of a totally hydraulic system. Extremely high pressures are required on the order of 30,000 psi. The elimination of the air supply could justify development along these lines for special operation.
3. The adaptation of the HP mechanism to other applications requiring an efficient high-speed linear actuator.

REFERENCES CITED

- Attewell, P.B., and Ramana, Y.V., 1965, Wave attenuation and internal friction as a function of frequency in rock: *Geophysics*, v. 31, p. 1049-1056.
- Bolt Associates, PAR* Output Signatures: published by Bolt Associates, Inc., Norwalk, Connecticut.
- Chelminski, P., 1975, personal communication: Bolt Associates, Inc., Norwalk, Connecticut.
- Farriol, R., Michon, D., Muniz, R., and Staron, P., Study and comparison of marine seismic signatures recorded in a very wide frequency band. Application to a new seismic source: the Vaporchoc*: Paper presented at the annual meeting of the Society of Exploration Geophysicists, New Orleans, Louisiana, November, 1970.
- Giles, B.F., and Johnston, R.C., 1973, Systems approach to air-gun array design: *Geophysical Prospecting*, v. 21, p. 77-101.
- Kramer, F.S., Peterson, R.A., and Walter, W.C., Seismic energy sources handbook 1968: Paper presented at the annual meeting of the Society of Exploration Geophysicists, Denver, Colorado, October, 1968, and private publication by Unived Geophysical Corporation. A subsidiary of the Bendix Corporation.
- Luskin, B., 1968, The PAR* air-gun: Paper presented at a symposium on Marine Non-Dynamite Energy Sources, sponsored by the Geophysical Society of Houston, April, 1968.
- ONR, 1965, Final report: steam sound source study: contract NO nr 4330(00), September, 1965, Raytheon Submarine Signal Division.
- Rayleigh, Lord, 1917, On the pressure developed in a liquid during the collapse of a spherical cavity: *Philosophical Magazine*, v. XXXIV, p. 94-98, 1917.
- Schempf, E.G., 1968, The HYDRO-SEIN*: Paper presented at a symposium on Marine Non-Dynamite Energy Sources sponsored by the Geophysical Society of Houston, April, 1968.
- Sodera, A guide to the Water Gun system: published by Société pour le développement de la recherche appliquée 9 bis, rue Jean Mallard-83100 Toulon, France.

APPENDIX

LIST OF NAMES AND TRADEMARKS

Casios Water Gun	Trademark Sodera Company, Toulon, France.
Hydro-Sein	Originally the Trademark of Marine Geophysical Services - Now a part of Western Geophysical Company of America.
Magnetic Air Gun	Trademark Bolt Associates, Norwalk, Connecticut.
MICA Water Gun	Trademark Sodera Company, Toulon, France.
PAR	Trademark Bolt Associates, Norwalk, Connecticut.
SEISMOJET	Trojan-U.S. Powder, Manufactured and Distributed by SIE-Dresser Systems.
Unipulse	Trademark Petty Geophysical Engineering Company, San Antonio, Texas